

# ornl

ORNL/TM-8290  
ENDF-326

OAK  
RIDGE  
NATIONAL  
LABORATORY

UNION  
CARBIDE

## Evaluated Neutron-Induced Cross Sections for $^{40}\text{Ca}$ from 20 to 40 MeV

D. M. Hetrick  
C. Y. Fu  
D. C. Larson

OPERATED BY  
UNION CARBIDE CORPORATION  
FOR THE UNITED STATES  
DEPARTMENT OF ENERGY

Printed in the United States of America. Available from  
National Technical Information Service  
U.S. Department of Commerce  
5285 Port Royal Road, Springfield, Virginia 22161  
NTIS price codes—Printed Copy: A05; Microfiche A01

*This report was prepared as an account of work sponsored by an agency of the United States Government. Neither the United States Government nor any agency thereof, nor any of their employees, makes any warranty, express or implied, or assumes any legal liability or responsibility for the accuracy, completeness, or usefulness of any information, apparatus, product, or process disclosed, or represents that its use would not infringe privately owned rights. Reference herein to any specific commercial product, process, or service by trade name, trademark, manufacturer, or otherwise, does not necessarily constitute or imply its endorsement, recommendation, or favoring by the United States Government or any agency thereof. The views and opinions of authors expressed herein do not necessarily state or reflect those of the United States Government or any agency thereof.*

ORNL/TM-8290  
ENDF-326

Engineering Physics Division

Evaluated Neutron-Induced Cross Sections for  $^{40}\text{Ca}$  from 20 to 40 MeV

D. M. Hetrick  
Computer Sciences

C. Y. Fu  
D. C. Larson  
Engineering Physics

Date Published - September 1982

OAK RIDGE NATIONAL LABORATORY  
Oak Ridge, Tennessee 37830  
operated by  
UNION CARBIDE CORPORATION  
for the  
U.S. DEPARTMENT OF ENERGY  
Under Contract No. W-7405-eng-26

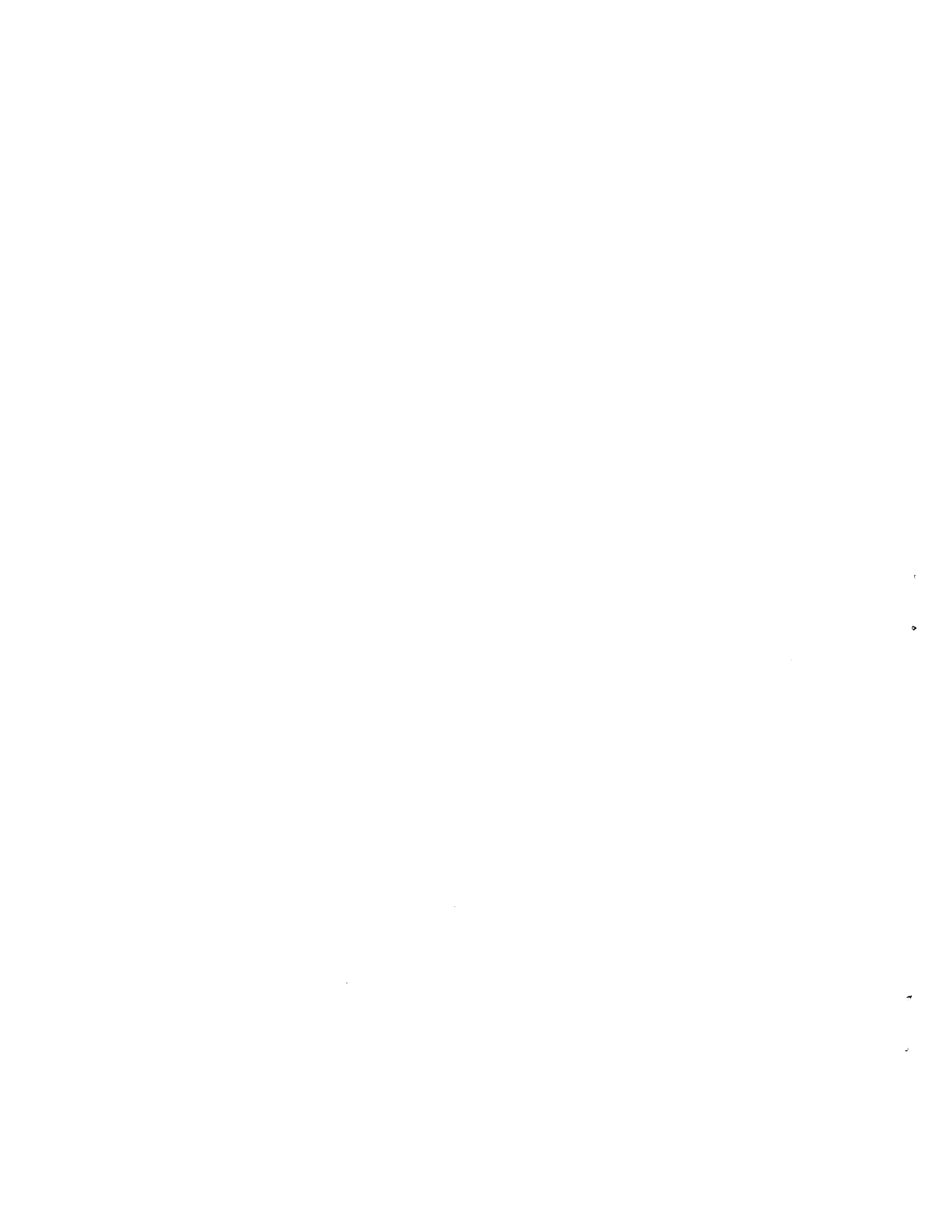
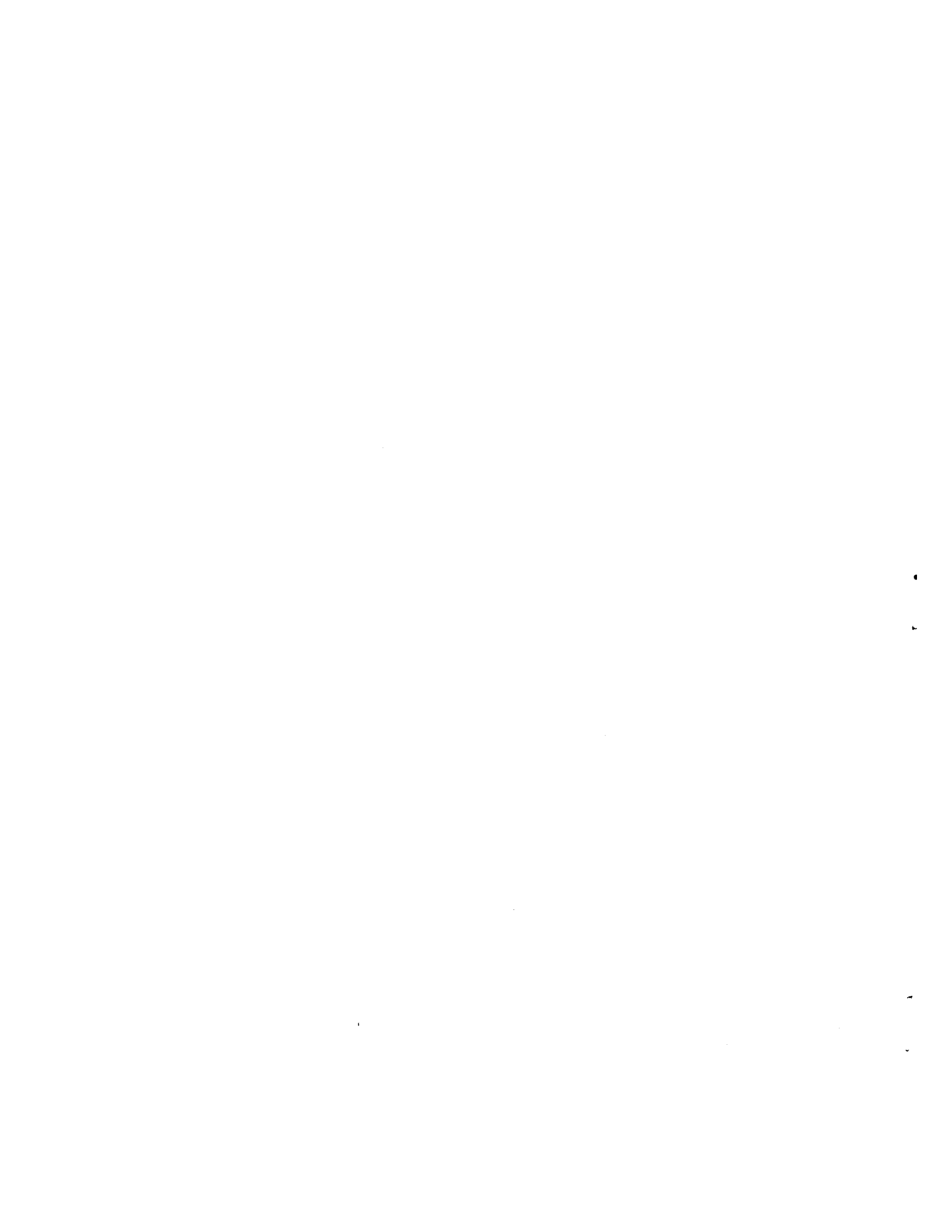


## TABLE OF CONTENTS

	Page
LIST OF TABLES. . . . .	v
LIST OF FIGURES . . . . .	vii
ACKNOWLEDGMENTS . . . . .	ix
ABSTRACT. . . . .	1
I. INTRODUCTION. . . . .	3
II. PARAMETER DETERMINATION . . . . .	5
Neutron Optical Model Potential . . . . .	5
Charged-Particle Optical Model Parameters . . . . .	11
Discrete Energy Levels and Level-Density Parameters . . . . .	13
The Direct Reaction Model and Parameters. . . . .	14
III. COMPUTATIONAL METHODS AND PROCEDURES. . . . .	27
IV. CALCULATED RESULTS. . . . .	29
V. THE EVALUATED FILE. . . . .	43
Reaction Type Labels. . . . .	43
(n,2n) Reaction . . . . .	45
(n,np) Reaction . . . . .	45
(n,n $\alpha$ ) Reaction . . . . .	46
Sum of Reactions. . . . .	46
Elastic . . . . .	46
(n,n') Discrete. . . . .	47
(n,n') Continuum. . . . .	47
Sum of (n,n') Discrete and Continuum. . . . .	47
(n,p) Reaction. . . . .	48
(n, $\alpha$ ) Reaction. . . . .	48
(n,d), (n,t), and (n, <sup>3</sup> He) Reactions . . . . .	48
Example of Format . . . . .	49
VI. SUMMARY . . . . .	51
REFERENCES. . . . .	53
APPENDIX - Example Listing of (n,np) Reaction in ENDF Format. . . . .	55



LIST OF TABLES

	Page
Table 1. Neutron Optical Model Parameters. . . . .	7
Table 2. Proton Optical Model Parameters . . . . .	12
Table 3. Alpha Optical Model Parameters. . . . .	12
Table 4. Energy Levels and Gamma-Ray Branching Ratios of $^{38}\text{K}$ . . . . .	15
Table 5. Energy Levels and Gamma-Ray Branching Ratios of $^{35}\text{Ar}$ . . . . .	16
Table 6. Energy Levels and Gamma-Ray Branching Ratios of $^{38}\text{Ca}$ . . . . .	16
Table 7. Energy Levels and Gamma-Ray Branching Ratios of $^{35}\text{Cl}$ . . . . .	17
Table 8. Energy Levels and Gamma-Ray Branching Ratios of $^{38}\text{Ar}$ . . . . .	18
Table 9. Energy Levels and Gamma-Ray Branching Ratios of $^{38}\text{Cl}$ . . . . .	19
Table 10. Energy Levels and Gamma-Ray Branching Ratios of $^{35}\text{S}$ . . . . .	20
Table 11. Energy Levels and Gamma-Ray Branching Ratios of $^{32}\text{P}$ . . . . .	21
Table 12. Energy Levels and Gamma-Ray Branching Ratios of $^{32}\text{S}$ . . . . .	23
Table 13. Energy Levels and Gamma-Ray Branching Ratios of $^{29}\text{Si}$ . . . . .	24
Table 14. Level Density Parameters. . . . .	25
Table 15. Reactions With Their Q-Values and New Descriptors . .	44





## LIST OF FIGURES

		Page
Figure 1.	Comparison of Final Optical Model Fit with Data of Ref. 6 (labeled OHIO) at 20 and 26 MeV. . . . .	8
Figure 2.	Comparison of Final Optical Model Fit with Data of Ref. 7 (labeled MSU) at 30.3 and 40 MeV . . . . .	9
Figure 3.	Comparison of Calculated Cross Sections from Optical Model with Data of Refs. 6 and 7 (Nonelastic), Refs. 6 and 7 (Elastic), and Ref. 9 (Total) . . . . .	10
Figure 4.	Composite of $n + {}^{40}\text{Ca}$ Cross Sections that Resulted from the Calculations . . . . .	31
Figure 5.	Calculated Neutron Emission Spectra for Incident Energies of 20 and 25 MeV . . . . .	32
Figure 6.	Calculated Neutron Emission Spectrum for Incident Energy of 30 MeV. . . . .	33
Figure 7.	Calculated Neutron Emission Spectra for Incident Energies of 35 and 40 MeV . . . . .	34
Figure 8.	Calculated Gamma-Ray-Production Cross Sections for Incident Energies of 20 and 25 MeV. . . . .	35
Figure 9.	Calculated Gamma-Ray-Production Cross Sections for Incident Energies of 30 and 35 MeV . . . . .	36
Figure 10.	Calculated Gamma-Ray-Production Cross Sections for Incident Energy of 40 MeV. . . . .	37
Figure 11.	Calculated Recoil Spectra ( ${}^{39}\text{K}$ residual) for Incident Energies of 20 and 25 MeV . . . . .	38
Figure 12.	Calculated Recoil Spectra ( ${}^{39}\text{K}$ residual) for Incident Energies of 30 and 35 MeV . . . . .	39

Figure 13.	Calculated Recoil Spectra ( $^{39}\text{K}$ residual) for Incident Energy of 40 MeV. . . . .	40
Figure 14.	Legendre Coefficients of the Calculated Angular Distributions for the First Outgoing Neutron in (n,nx) Reaction for Incident Energies Between 20 and 40 MeV. . . . .	41

## ACKNOWLEDGMENTS

We are grateful to Betty Waddell for typing this report. Many helpful comments and suggestions were received from J. K. Dickens and R. W. Roussin, who reviewed the manuscript. This research was sponsored by the Offices of Fusion Energy and Basic Energy Science.



## ABSTRACT

Nuclear model codes were used to compute cross sections for neutron-induced reactions on  $^{40}\text{Ca}$  for incident energies from 20 to 40 MeV. The input parameters for the model codes were determined through analysis of experimental data in this energy region. Computed cross sections along with emission spectra for each product were combined into an Evaluated Nuclear Data File (ENDF) using the proposed format for charged-particle reactions. Discussion of the models used, the resulting calculations, and the final evaluated data file are included in this report.



## I. INTRODUCTION

The Fusion Materials Irradiation Test Facility (FMIT) requires evaluated neutron cross sections for many elements (or materials) up to incident energies of around 40 MeV.<sup>1</sup> An important material for which data are needed is calcium, a constituent of concrete. Recently, new calculations<sup>2</sup> of cross sections were performed for  $^{40}\text{Ca}$  up to incident energies of 20 MeV, and these cross sections were included in the Evaluated Nuclear Data File (ENDF). This report documents calculations of cross sections that were made using nuclear model codes for neutron reactions on  $^{40}\text{Ca}$  for incident energies of 20 to 40 MeV. Care was taken to ensure continuity with the previous evaluation<sup>2</sup> at the incident energy of 20 MeV. These new calculations were included in a separate data file using the proposed ENDF charged particle format.<sup>3</sup>

With the exception of the total cross section and some elastic scattering angular distributions, very little neutron-induced experimental data exist above 20 MeV. Thus, most of this evaluation depended on results determined from nuclear-model code calculations. The Hauser-Feshbach code TNG1<sup>4</sup>, an upgraded version of TNG,<sup>5</sup> was used in this evaluation. TNG1 accounts for energy and angular distributions of particles emitted in the precompound reaction, ensures consistency for all reactions, and maintains energy balance.

The optical model parameter sets, discrete energy levels, and other parameters needed as input for TNG1 are discussed in Chapter II. Chapter III includes a discussion of the computational methods and procedures for the calculations. Figures showing calculated results are given in Chapter IV along with some brief discussions. In Chapter V, we discuss the new evaluated file format<sup>3</sup> and how this evaluation was constructed. A short summary is given in Chapter VI. The resulting data set has been transmitted to the National Nuclear Data Center at Brookhaven National Laboratory for inclusion in ENDF/B.





## II. PARAMETER DETERMINATION

### Neutron Optical Model Potential

Since this evaluation depends heavily on nuclear model calculations, much effort was spent to determine a good set of neutron optical model parameters for  $n + {}^{40}\text{Ca}$ . The final potential should reproduce the elastic scattering angular distribution data available, as well as the nonelastic, elastic and total cross sections. Since the model calculations require transmission coefficients for energies less than 20 MeV, the neutron optical potential studies included data for incident energies from 4 to 40 MeV. In particular, angular distribution data used in the present analysis include those used for the evaluation of Ref. 5, supplemented by the angular distribution data of Rapaport et al.<sup>6</sup> at 11, 20 and 26 MeV, and data of DeVito et al.<sup>7</sup> at 30.3 and 40 MeV. Total elastic scattering cross sections were obtained by integrating each of the angular distribution data sets. Wick's theorem<sup>8</sup> was used to estimate the cross section at  $0^\circ$ , and since none of the data sets cover the angular range to  $180^\circ$ , three extra data points were added between  $\theta_{\text{max}}$  of the measurement and  $180^\circ$ , spaced equally in angle and all with the cross section value measured at  $\theta_{\text{max}}$ . The added data point at  $0^\circ$  was given an uncertainty of 5%, while the three added points at larger angles were given uncertainties of 50%. These added points were used to help constrain the least-squares fit during extraction of the total elastic cross section, but were not used during the remainder of the analysis. The total cross section values were taken from recent work of Larson et al.<sup>9</sup> The nonelastic cross sections were then extracted by subtracting the total elastic cross sections from the total cross section. Individual best-fit parameters were then obtained for each of the angular distribution data sets, using the code GENOA,<sup>10</sup> and searching techniques similar to those for the evaluation for  $E_n \leq 20$  MeV as described in Ref. 5. A compound elastic angular distribution term was included, with an energy dependent magnitude included as a search variable. For energies  $E_n \geq 15$  MeV, the compound elastic term is very small and was not included in the present evaluation. Following the individual searches, an average

geometry was obtained by averaging the results of the individual searches, weighted by  $1/|x|$ . With the average geometry thus determined, individual searches were again done, this time only on the strengths of the real and surface-imaginary terms  $V$  and  $W_D$ . A linear least-squares analysis was used to determine an energy dependence for the strengths. In preliminary work, the volume absorption was found to be poorly determined by the angular distribution data, and its final form was chosen and fixed prior to the last search on strengths by adjusting it to reproduce the total cross section up to 80 MeV. Parameters for the best-fit parameter set finally obtained from this work are given in Table 1. Comparing results using this potential with the Ca potential used for the evaluation of Ref. 5, we find that fits to the angular distribution data, for  $E_n$  between 4 and 15 MeV are essentially equivalent. However, from 20 to 40 MeV the new potential provides significantly better fits to the angular distribution data of Refs. 6 and 7. Figs. 1 and 2 show a comparison of our calculated results with measured data at 20, 26, 30.3 and 40 MeV, while Fig. 3 shows a comparison of the calculated total, elastic and nonelastic cross sections with the measured total, and extracted elastic and nonelastic cross sections. Agreement is satisfactory at least up to 40 MeV, which is the upper limit of this evaluation.

Table 1. Neutron Optical Model Parameters

---

$V(\text{MeV})$	$= 52.42 - 0.26E$	
$W(\text{MeV})$	$= -5.0 + 0.17E$ , or 0.0 whichever is greater	
$W_D(\text{MeV})$	$= 4.35 + 0.20E$ for $E \leq 17.6$ MeV	
	$= 8.77 - 0.051E$ for $E > 17.6$ MeV	
$U(\text{MeV})$	$= 6.2$	
$r_V(\text{fm})$	$= 1.198$	$a_V(\text{fm}) = 0.696$
$r_W(\text{fm})$	$= 1.263$	$a_W(\text{fm}) = 0.596$
$r_U(\text{fm})$	$= 1.01$	$a_U(\text{fm}) = 0.75$

---

$E$  = incident energy (MeV)

$V$  = real well depth

$W$  = imaginary well depth (Wood-Saxon)

$W_D$  = imaginary well depth (Wood-Saxon derivative)

$U$  = spin-orbit potential depth

$r_V, r_W, r_U$  = radii for various potentials

$a_V, a_W, a_U$  = diffuseness for various potentials

ORNL-DWG 82-15853

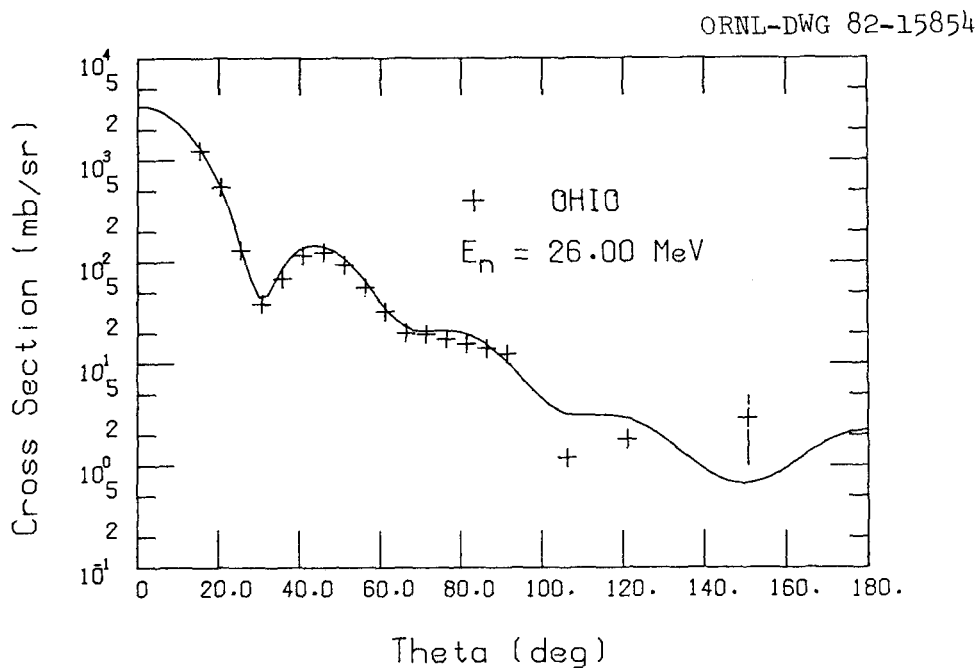
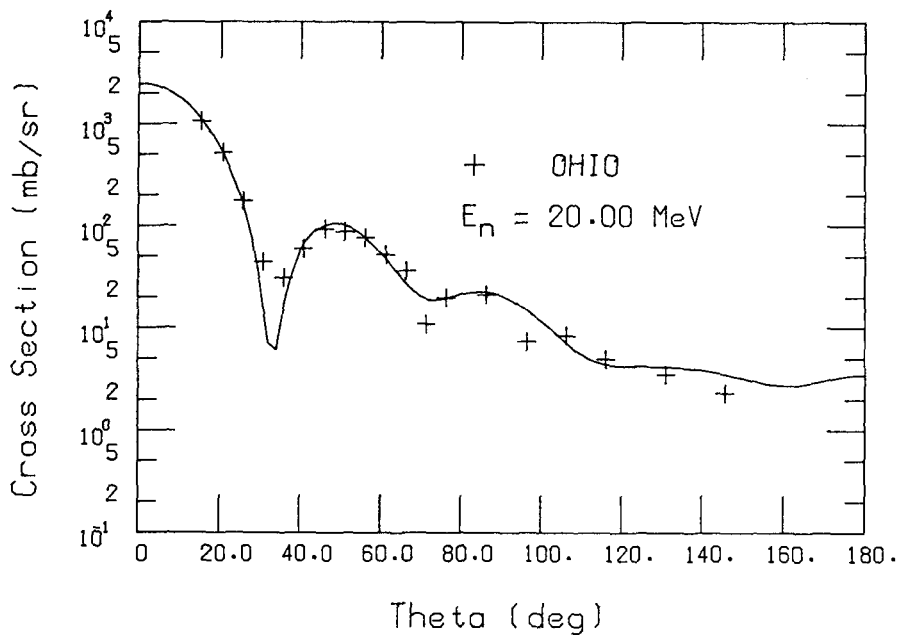


Figure 1. Comparison of Final Optical Model Fit with Data of Ref. 6 (labeled OHIO) at 20 and 26 MeV

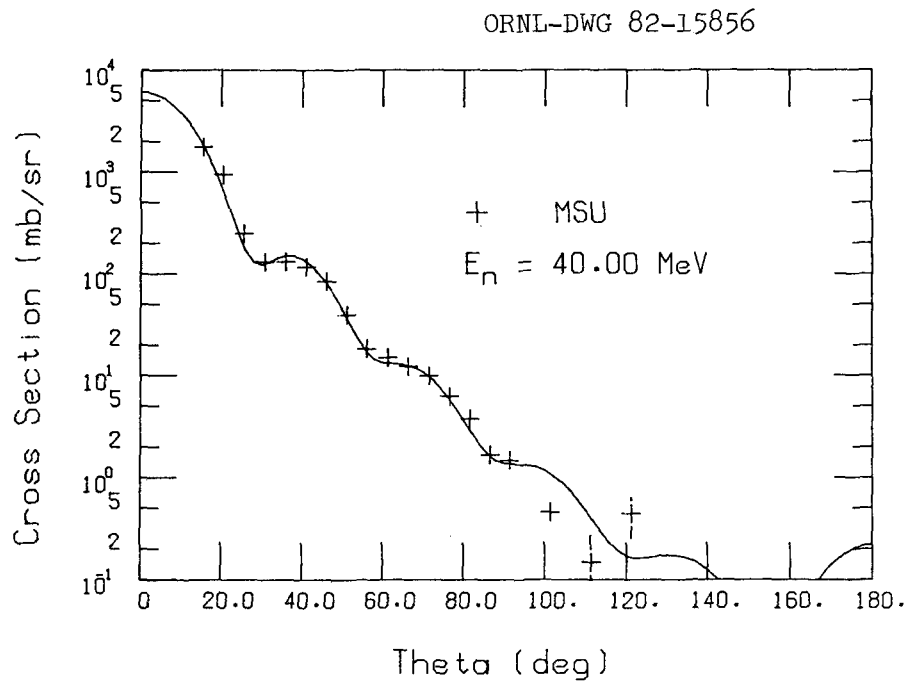
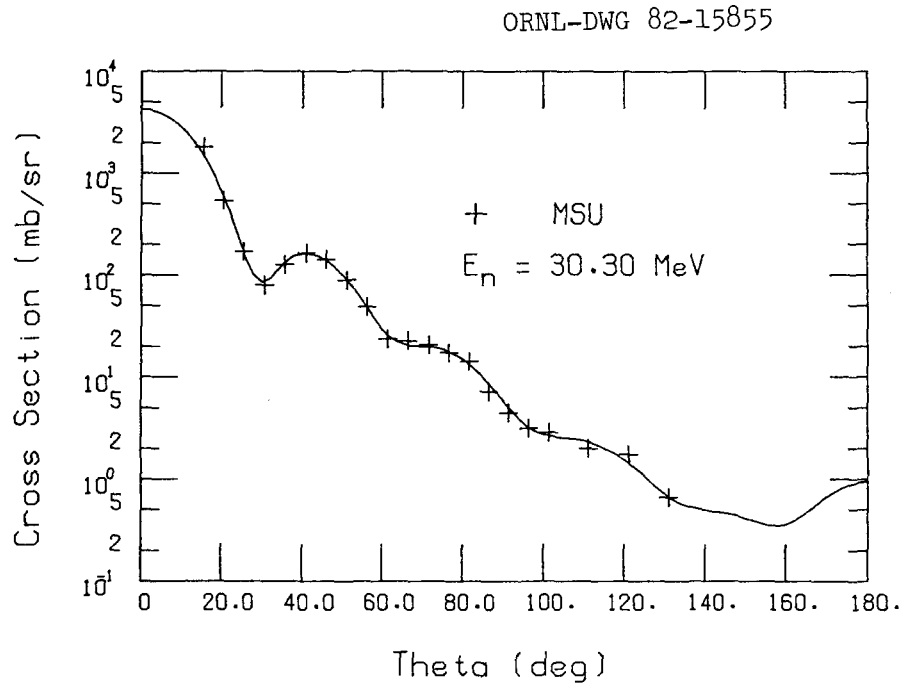


Figure 2. Comparison of Final Optical Model Fit with Data of Ref. 7 (labeled MSU) at 30.3 and 40 MeV

ORNL-DWG 82-15857

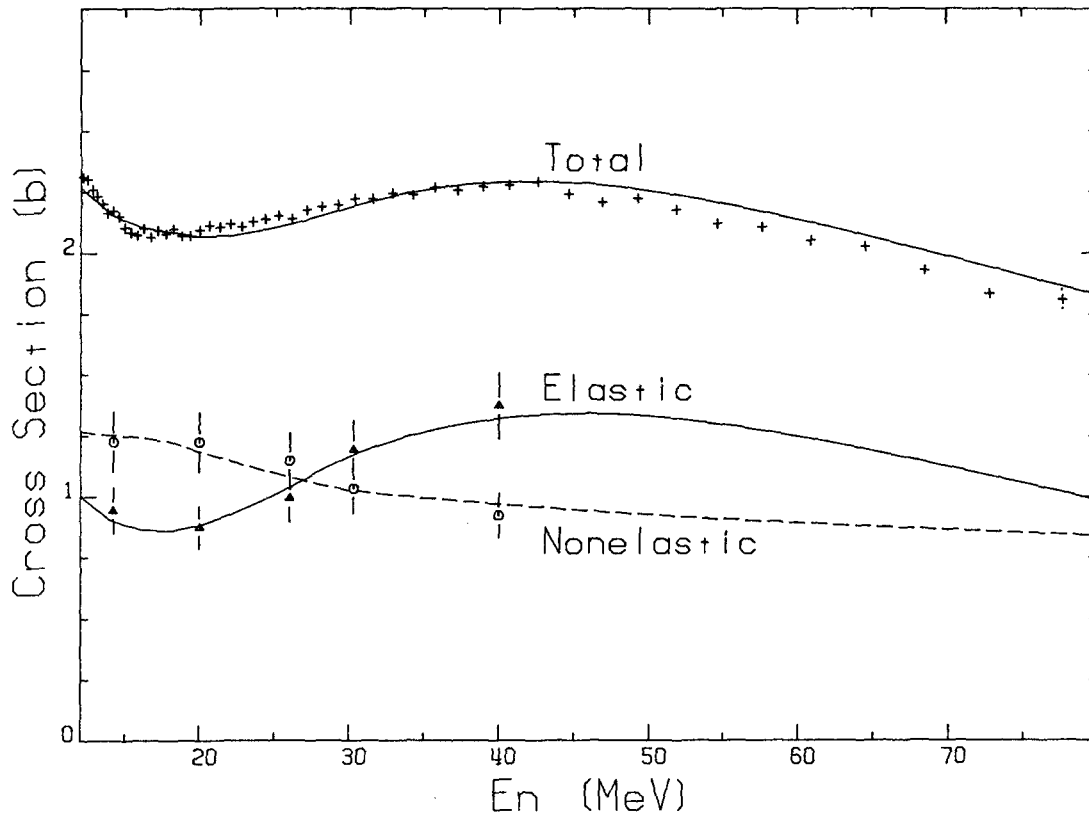


Figure 3. Comparison of Calculated Cross Sections from Optical Model with Data of Refs. 6 and 7 (Nonelastic), Refs. 6 and 7 (Elastic), and Ref. 9 (Total)

### Charged-Particle Optical-Model Parameters

The proton optical-model parameters are taken from the work of Gruhn et al.<sup>11</sup> They measured elastic scattering from  $^{40}\text{Ca}$  at 25, 30, 35 and 40 MeV. Their optical model analysis used the geometry determined by Fricke et al.<sup>12</sup> in a global analysis of proton scattering, but they allowed the strengths of the real and imaginary potentials to vary. A linear least-squares analysis was done on their real potential strengths to determine a linear energy dependence, and the strengths of the absorption potentials were simply averaged. The resulting optical model potential used for the protons is given in Table 2.

Optical model parameters for alpha particles were taken as set number 4 from the work of McFadden and Satchler.<sup>13</sup> They are given in Table 3.

Table 2. Proton Optical Model Parameters\*

---

$V(\text{MeV}) = 56.46 - 0.293E$	$r_V(\text{fm}) = 1.16$	$a_V(\text{fm}) = 0.75$
$W(\text{MeV}) = 2.29$	$r_W(\text{fm}) = 1.37$	$a_W(\text{fm}) = 0.63$
$W_D(\text{MeV}) = 4.21$		
$U(\text{MeV}) = 6.04$	$r_U(\text{fm}) = 1.064$	$a_U(\text{fm}) = 0.738$

---

\*Parameter definitions are as in Table 1.

Table 3. Alpha Optical Model Parameters\*

---

$V(\text{MeV}) = 195.0$	$r_V(\text{fm}) = 1.21$	$a_V(\text{fm}) = 0.721$
$W(\text{MeV}) = 0.0$	$r_W(\text{fm}) = 1.21$	$a_W(\text{fm}) = 0.721$
$W_D(\text{MeV}) = 19.2$		

---

\*Parameter definitions are as in Table 1.



### Discrete Energy Levels and Level-Density Parameters

The model calculations require a complete description of the energy levels of the residual nuclei for the various open channels. The low-energy region of excitation of these nuclei can be adequately described in terms of discrete levels for which we usually know the energy, spin and parity ( $J^\pi$ ), and gamma-ray deexcitation branching ratios, hereinafter referred to as branching ratios. As the excitation energy increases, our knowledge of these levels becomes incomplete; and eventually, as their number increases, we prefer to describe them in terms of a level density formula. Since it was necessary to maintain continuity at 20 MeV for the reaction cross sections, the level energies, spins, parities, and deformation parameters for the nuclei  $^{40}\text{Ca}$ ,  $^{40}\text{K}$ ,  $^{37}\text{Ar}$ ,  $^{39}\text{K}$ ,  $^{36}\text{Ar}$ ,  $^{39}\text{Ar}$ ,  $^{36}\text{Cl}$ ,  $^{33}\text{S}$ , and  $^{39}\text{Ca}$ , needed for the reactions (n,n'), (n,p), (n, $\alpha$ ), (n,np), (n,n $\alpha$ ), (n,2p), (n,p $\alpha$ ), (n,2 $\alpha$ ), and (n,2n), respectively, were as used in the calculations for the evaluation to 20 MeV.<sup>2</sup> However, in extending the calculations up to incident energies of 40 MeV, level information for the additional nuclei  $^{38}\text{Ca}$ ,  $^{38}\text{K}$ ,  $^{35}\text{Ar}$ ,  $^{38}\text{Ar}$ ,  $^{35}\text{Cl}$ ,  $^{32}\text{S}$ ,  $^{38}\text{Cl}$ ,  $^{35}\text{S}$ ,  $^{32}\text{P}$ , and  $^{29}\text{Si}$ , were needed for the reactions (n,3n), (n,2np), (n,2n $\alpha$ ), (n,n2p), (n,np $\alpha$ ), (n,n2 $\alpha$ ), (n,3p), (n,2p $\alpha$ ), (n,p2 $\alpha$ ), and (n,3 $\alpha$ ), respectively.

For the above additional nuclei, the level energies, their  $J^\pi$  values and gamma-ray branching ratios adopted are given in Tables 4 to 13. All values given in these tables were taken from Endt and Van der Leun.<sup>14</sup> Because the cross sections for these nuclei are dominated by the excitation of the low-lying energy levels, only the low-lying levels with fairly well-established  $J^\pi$  values were included. There are levels where the energies are known, but  $J^\pi$  values and/or branching ratios are experimentally undetermined. These  $J^\pi$  values and branching ratios were assigned as indicated by the parentheses in the Tables. Some of these assigned values were suggested by Endt and Van der Leun.<sup>14</sup> In most cases, excited states were reported by Endt and Van der Leun<sup>14</sup> having  $E_x$  larger than for levels shown in Tables 4-13. However, the branching ratios for these higher levels were not known and thus were not used in the calculations.

To represent the continuum excitation energy region occurring above the last discrete level (continuum cutoff  $E_c$ ), the level density formulae as described by Fu<sup>4,5</sup> were used. The level density parameters used for those nuclei analyzed in the calculations for  $E_n \leq 20$  MeV are given in Ref. 2. The level density parameters for the additional residual nuclei analyzed in the calculations for  $20 \leq E_n \leq 40$  MeV are given in Table 14.

#### The Direct Reaction Model and Parameters

The Distorted Wave Born Approximation (DWBA) program DWUCK<sup>15</sup> was used to calculate the direct-interaction component of the inelastic-scattering cross sections. Inputs to this code were the neutron optical-model parameters of Table 1 and the deformation parameters,  $\beta_\ell$ , determined for the evaluation for  $E_n \leq 20$  MeV given in Ref. 5. The resulting calculated direct inelastic excitation cross sections were used as input in the TNG1 code<sup>4</sup> to compute gamma-ray spectra.

Table 4. Energy Levels and Gamma-Ray Branching Ratios of  $^{38}\text{K}$ 

Initial State			Branching Ratios to State N							
N	J <sup><math>\pi</math></sup>	E(keV)	1	2	3	4	5	6	7	13
1	3 <sup>+</sup>	0								
2	0 <sup>+</sup>	130	*							
3	1 <sup>+</sup>	459	1	99						
4	1 <sup>+</sup>	1698		100						
5	2 <sup>+</sup>	2402		6	94					
6	3 <sup>-</sup>	2613	100							
7	(2) <sup>-</sup>	2646	99		1					
8	1 <sup>-</sup>	2829		90			10			
9	2 <sup>-</sup>	2870	42		31	11	16			
10	0 <sup>-</sup>	2993			100					
11	(1 <sup>+</sup> )	3316	43				57			
12	1 <sup>+</sup>	3342		100						
13	(4) <sup>-</sup>	3420	42						58	
14	2 <sup>+</sup>	3431	40				60			
15	(5) <sup>+</sup>	3458							19	81
16	(1) <sup>-</sup>	3615							100	
17	3 <sup>+</sup>	3668					100			

\* positron emission

Table 5. Energy Levels and Gamma-Ray Branching Ratios of  $^{35}\text{Ar}$ 

Initial State			Branching Ratios to State N	
N	$J^\pi$	E(keV)	1	
1	$3/2^+$	0		
2	$1/2^+$	1184	100	
3	$(3/2)^+$	1750	100	
4	$3/2^+$	2600	100	

Table 6. Energy Levels and Gamma-Ray Branching Ratios of  $^{38}\text{Ca}$ 

Initial State			Branching Ratios to State N	
N	$J^\pi$	E(keV)	1	2
1	$0^+$	0		
2	$2^+$	2206	100	
3	$0^+$	3050		100
4	$2^+$	3690	52	48

Table 7. Energy Levels and Gamma-Ray Branching Ratios of  $^{35}\text{Cl}$ 

Initial State			Branching Ratios to State N						
N	$J^\pi$	E(keV)	1	2	3	4	5	6	7
1	$3/2^+$	0							
2	$1/2^+$	1219	100						
3	$5/2^+$	1763	100						
4	$7/2^+$	2645	91		9				
5	$3/2^+$	2694	79	8	13				
6	$5/2^+$	3003	100						
7	$7/2^-$	3163	90		.3	8		1.7	
8	$3/2^+$	3918	82		18				
9	$9/2^+$	3943			92	8			
10	$1/2^+$	3968	20	78			2		
11	$3/2^-$	4059		94	5		1		
12	$7/2^+$	4113	52		48				
13	$5/2^-$	4173	58		16		26		
14	$3/2^-$	4178	61	31			8		
15	$9/2^-$	4347				33			67
16	$(5/2^+)$	4624	100						

Table 8. Energy Levels and Gamma-Ray Branching Ratios of  $^{38}\text{Ar}$ 

Initial State			Branching Ratios to State N										
N	$J^\pi$	E(keV)	1	2	3	4	5	6	7	8	9	10	11
1	$0^+$	0											
2	$2^+$	2168	100										
3	$0^+$	3377		100									
4	$3^-$	3810		100									
5	$2^+$	3937	94	6									
6	$4^-$	4480				100							
7	$2^+$	4565		96		2	2						
8	$5^-$	4586				10		90					
9	$0^+$	4710					100						
10	$3^-$	4877		46		54							
11	$(1)^-$	5084		94		6							
12	$2^+$	5157	9	54		13	24						
13	$4^+$	5350		59		9	32						
14	$3^-$	5513		29		11		37				23	
15	$(1)^+$	5552	12	26			39		23				
16	$2^+$	5595	23		17		37		23				
17	$5^-$	5658				2		9		89			
18	$1^-$	5734	100										
19	$3^-$	5825		17		35		12				25	11

Table 9. Energy Levels and Gamma-Ray Branching Ratios of  $^{38}\text{Cl}$ 

Initial State			Branching Ratios to State N							
N	$J^\pi$	E(keV)	1	2	3	4	5	6	7	8
1	$2^-$	0								
2	$5^-$	671	100							
3	$3^-$	755	100							
4	$4^-$	1309	6	76	18					
5	$3^-$	1617	19	3	28	50				
6	$(1)^-$	1692	93		7					
7	$(0)^-$	1746	100							
8	$(2)^-$	1785			100					
9	$1^+$	1942	100							
10	$(2)^-$	1981	44		24		22	10		
11	$3^-$	2743	19		9	33	14			25
12	$1^+$	2752	(100)							
13	$(0)^-$	2895	100							

Table 10. Energy Levels and Gamma-Ray Branching Ratios of  $^{35}\text{S}$ 

Initial State			Branching Ratios to State N	
N	$J^\pi$	E(keV)	1	2
1	$3/2^+$	0		
2	$1/2^+$	1572	100	
3	$7/2^-$	1991	100	
4	$3/2^-$	2348	73	27
5	$5/2^+$	2718	100	
6	$(3/2)^+$	2939	100	
7	$5/2^+$	3421	100	



Table 11. Energy Levels and Gamma-Ray Branching Ratios of  $^{32}\text{P}$ 

Initial State			Branching Ratios to State N										
N	$J^\pi$	E(keV)	1	2	3	4	5	6	7	8	9	10	14
1	$1^+$	0											
2	$2^+$	78	100										
3	$0^+$	513	100										
4	$1^+$	1150	7	43	50								
5	$2^+$	1323	59	41									
6	$3^+$	1755	2	96				2					
7	$2^+$	2178	9	91									
8	$2^+$	2219	47	12		9	32						
9	$1^+$	2230	19	81									
10	$2^+$	2658	78	22									
11	$1^+$	2745	26		74								
12	$3^+$	3005	7	85				4			4		
13	$4^+$	3149		7				60	13	20			
14	$2^-$	3264	3	14		44	17	12				10	
15	$3^-$	3322		75			25						
16	$4^-$	3443							94	6			
17	$(0^+)$	3445	39	44								17	
18	$3^+$	3797		22				78					
19	$2^+$	3880	68	32									
20	$(1^+)$	3990		84						16			
21	$2^-$	4007	40	40									20
22	$4^+$	4035		35						65			
23	$1^-$	4036		5	76	19							



Table 12. Energy Levels and Gamma-Ray Branching Ratios of  $^{32}\text{S}$ 

Initial State			Branching Ratios to State N	
N	$J^\pi$	E(keV)	1	2
1	$0^+$	0		
2	$2^+$	2230	100	
3	$0^+$	3778		100
4	$2^+$	4782	86	14
5	$4^+$	4459		100
6	$1^+$	4695	40	60
7	$3^-$	5006	3	97
8	$3^+$	5413		100
9	$2^+$	5549	40	60
10	$1^-$	5798	100	
11	$2^-$	6224		100
12	$4^+$	6411		100

Table 13. Energy Levels and Gamma-Ray Branching Ratios of  $^{29}\text{Si}$ 

Initial State			Branching Ratios to State N										
N	$J^\pi$	E(keV)	1	2	3	4	5	6	7	8	9	11	
1	$1/2^+$	0											
2	$3/2^+$	1273	100										
3	$5/2^+$	2028	94	6									
4	$3/2^+$	2426	87	13									
5	$5/2^+$	3067		80	20								
6	$7/2^-$	3624		2	89		9						
7	$7/2^+$	4080		68	32								
8	$9/2^+$	4741			93				7				
9	$1/2^+$	4840	90	10									
10	$5/2^+$	4895	18	50	32								
11	$3/2^-$	4934	94	6									
12	$9/2^-$	5255						100					
13	$7/2^+$	5286		11	76	13							
14	$9/2^+$	5652					41		47	12			
15	$7/2^+$	5813			25	30	45						
16	$3/2^+$	5949	14	23	15	22	26						
17	$(3/2^+)$	6107			78	22							
18	$7/2^-$	6191			100								
19	$1/2^-$	6381	63	20		11					2	4	

Table 14. Level Density Parameters

Residual Nuclei	T (MeV)	$E_o$ (MeV)	a (MeV <sup>-1</sup> )	$\Delta$ (MeV)	c	$E_c$ (MeV)	$E_x$ (MeV)
<sup>38</sup> K	1.518	-1.850	5.124	0.00	5.143	3.687	6.447
<sup>35</sup> Ar	1.710	-0.235	4.405	1.62	4.186	2.980	8.406
<sup>38</sup> Ca	1.632	1.981	4.608	3.69	4.626	3.695	10.137
<sup>35</sup> Cl	1.580	-0.154	4.950	1.86	4.703	4.768	8.646
<sup>38</sup> Ar	1.424	1.684	5.636	3.66	5.657	5.858	10.107
<sup>38</sup> Cl	1.330	-2.110	6.246	0.00	6.269	2.950	6.447
<sup>35</sup> S	1.517	-0.477	5.259	1.62	4.997	3.561	8.406
<sup>32</sup> P	1.708	-2.140	4.535	0.00	4.059	4.412	7.188
<sup>32</sup> S	1.714	2.000	4.066	3.29	3.639	6.620	8.915
<sup>29</sup> Si	1.892	-0.175	4.022	2.09	3.371	6.420	9.762

(See Refs. 4,5,16 for formulae.)

T = nuclear temperature

$E_o$  = parameter for matching lower energy density to the higher one

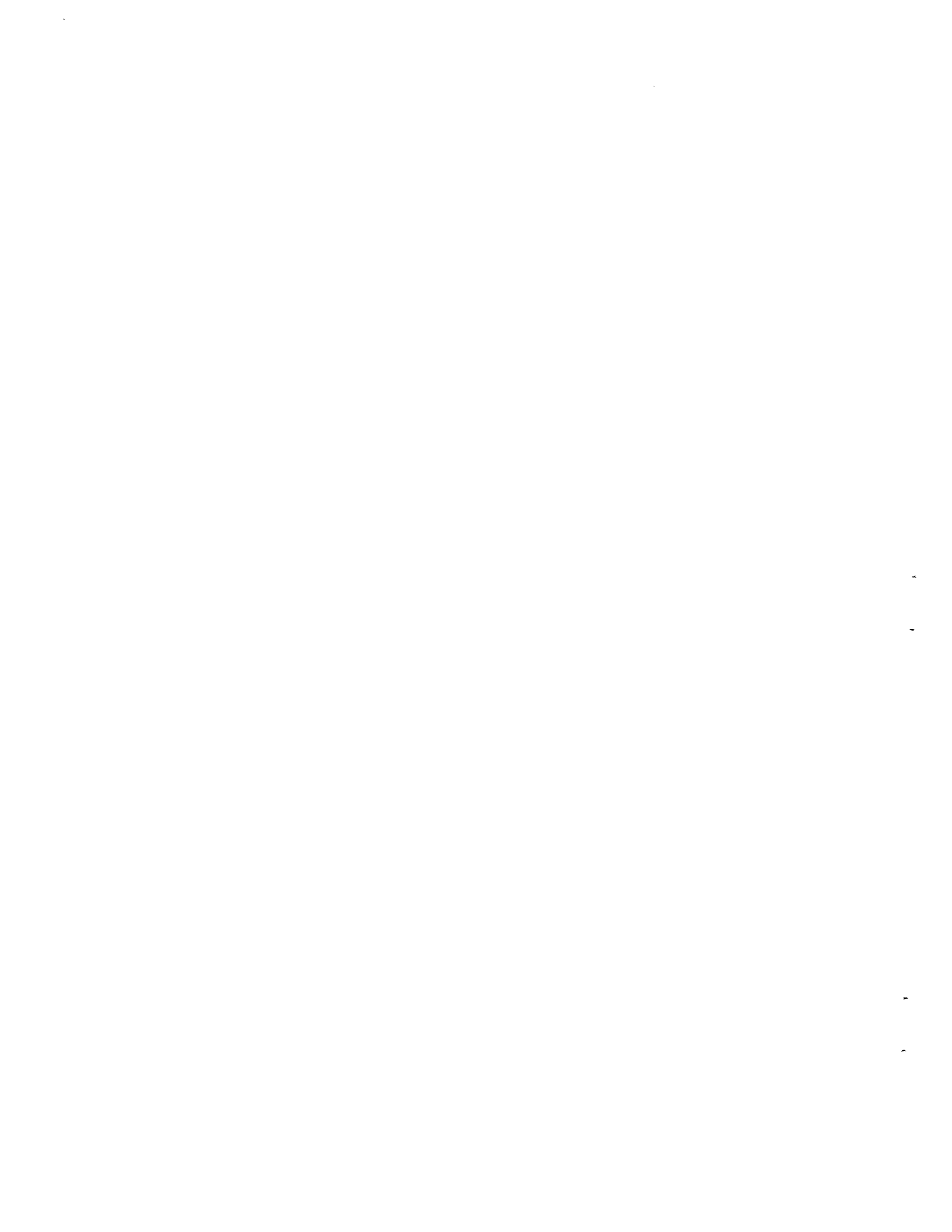
a =  $\pi^2 g/6$  (g = density of uniformly spaced single particle states)

$\Delta$  = pairing energy correction

c = spin cutoff parameter

$E_c$  = continuum cutoff

$E_x$  = tangency point



### III. COMPUTATIONAL METHODS AND PROCEDURES

In view of the lack of experimental data for the reaction channels which are open, this evaluation could not have been performed without very extensive theoretical analyses. The present analyses make use of the model code TNG1.<sup>4</sup> Parameters required as input to TNG1 are now summarized. The discrete energy levels for each of the residual nuclei and the gamma-ray branching ratios (Tables 4-13 and Ref. 2), the level density parameters (Table 14 and Ref. 2), the direct inelastic cross sections calculated by DWUCK<sup>15</sup> (see Section II), and the optical model parameters (Tables 1 - 3) were all used as input to the TNG1 computer code. Parameters required for the precompound mode of reaction were the same as determined previously in a global analysis.<sup>4</sup>

TNG1 simultaneously computes the binary-reaction, tertiary reaction, and resulting gamma-ray production cross sections. Calculations were carried to the third step in the multistep Hauser-Feshbach model. For example, complex chains such as  $(n,n2p)$  [(sum of  $(n,2pn) + (n,pnp) + (n,n2p)$ ] are important (see next section) in the decay process and were included in the calculations. Also, TNG1 computes the compound and precompound cross sections in a consistent fashion and conserves angular momentum in both compound and precompound reactions. Thus, the cross section sets are consistent and energy balance is ensured.

Since the main use of this evaluation is foreseen to be in neutron transport calculated through concrete, emphasis has been given to the neutron emission cross sections. The reactions which result in emission of charged particles have been calculated, with the partial cross sections being combined, as the individual reaction cross sections are assumed not to be needed separately.





#### IV. CALCULATED RESULTS

Other than experimental data shown in Figs. 1-3, there are no existing data with which to compare calculated results for Ca above incident energies of 20 MeV. In this section we show calculated results.

A summary of the reaction cross sections obtained from the calculations is given in Fig. 4. The reaction cross section curve labeled (n,other) includes the sum of the following calculated cross sections:

(n,2 $\alpha$ ),  
(n, $\alpha$ p) [sum of (n,p $\alpha$ ) + (n, $\alpha$ p)],  
(n,3n),  
(n,2np) [sum of (n,npn) + (n,p2n) + (n,2np)],  
(n,2n $\alpha$ ) [sum of (n,n $\alpha$ n) + (n, $\alpha$ 2n) + (n,2n $\alpha$ )],  
(n,n2 $\alpha$ ) [sum of (n,n2 $\alpha$ ) + (n, $\alpha$ n $\alpha$ ) + (n,2 $\alpha$ n)],  
(n,n2p) [sum of (n,2pn) + (n,n2p) + (n,pnp)],  
(n,np $\alpha$ ) [sum of (n,np $\alpha$ ) + (n,n $\alpha$ p) + (n,pn $\alpha$ ) + (n,p $\alpha$ n) +  
(n, $\alpha$ np) + (n, $\alpha$ pn)],  
(n, $\alpha$ 2p) [sum of (n,2p $\alpha$ ) + (n,p $\alpha$ p) + (n, $\alpha$ 2p)],  
(n,p2 $\alpha$ ) [sum of (n,p2 $\alpha$ ) + (n, $\alpha$ p $\alpha$ ) + (n,2 $\alpha$ p)],  
(n,3 $\alpha$ ), and  
(n,2p).

We mention here that there were no MT numbers assigned to many of the above reactions in the proposed format.<sup>3</sup> Others have small contributions, and thus, to shorten the evaluated file, the above reactions were added together. In this case, the yields and energy distributions for each incident energy and for each outgoing particle were put into the file. Thus, if needed, the neutron emission spectrum can be retrieved. In particular, the summed cross sections above, the neutron yield, and the energy distribution were retrieved and used in calculating the total neutron emission spectrum (see below). Fig. 4 illustrates that processes involving complex chains such as those listed above do become important at higher incident energies.

Figs. 5 - 7 show the calculated total neutron emission spectra for incident energies of 20, 25, 30, 35, and 40 MeV, respectively. The calculated gamma-ray production cross sections for incident energies of 20, 25, 30, 35, and 40 MeV are shown in Figs. 8 - 10. The recoil spectra from the (n,np) reaction ( $^{39}\text{K}$  residual) for incident energies 20, 25, 30, 35, and 40 MeV are shown in Figs. 11 - 13. The recoil spectra from other reactions are not shown here since they have much the same shapes as those from the (n,np) reaction.

The angular distributions of the first outgoing neutron were calculated according to the method described by Fu<sup>17</sup> for the compound and precompound reactions. The Legendre coefficients of the calculated angular distributions are shown in Fig. 14. The calculated results show only a weak dependence on the energy of the incident neutron. Therefore, we assumed that these distributions are independent of the energy of the incident neutron. The angular distributions for the second and third outgoing neutrons are assumed to be isotropic. Angular distributions for the outgoing charged particles are believed not useful for applications involving calcium and are therefore given as isotropic. The next section describes how the angular distributions for the neutrons were entered into the evaluated file.

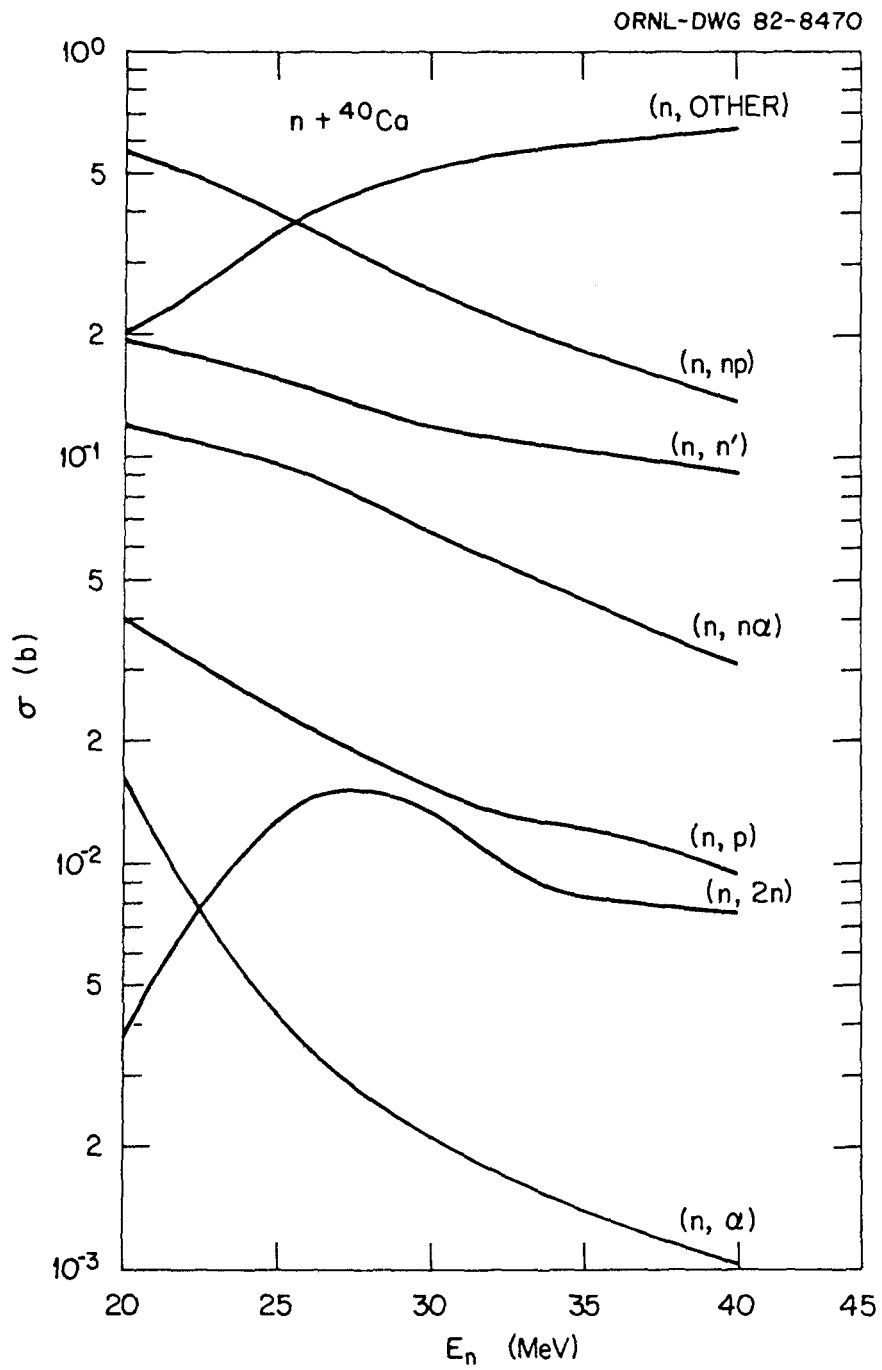
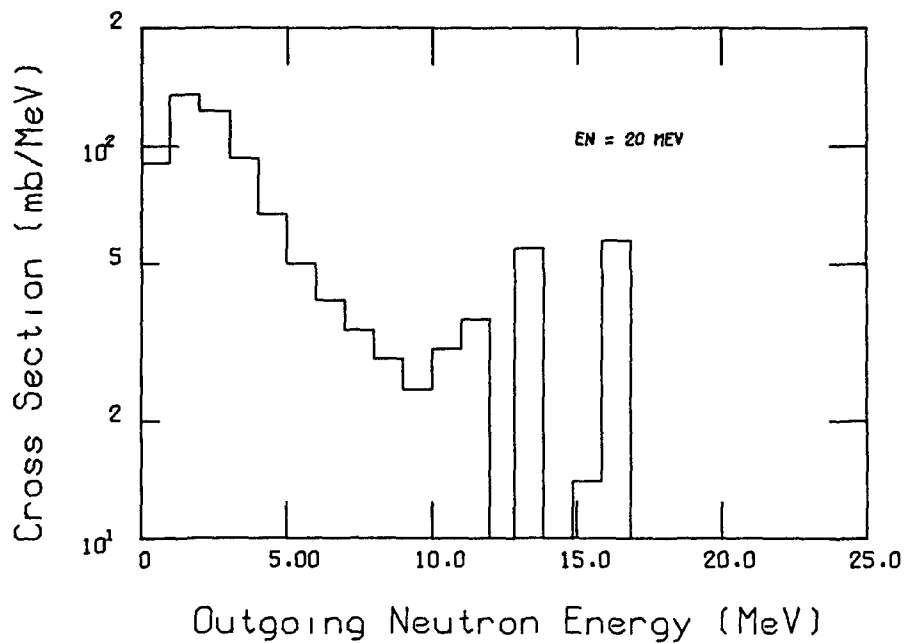


Figure 4. Composite of  $n + {}^{40}\text{Ca}$  Cross Sections that Resulted from the Calculations

ORNL-DWG 82-15858



ORNL-DWG 82-15859

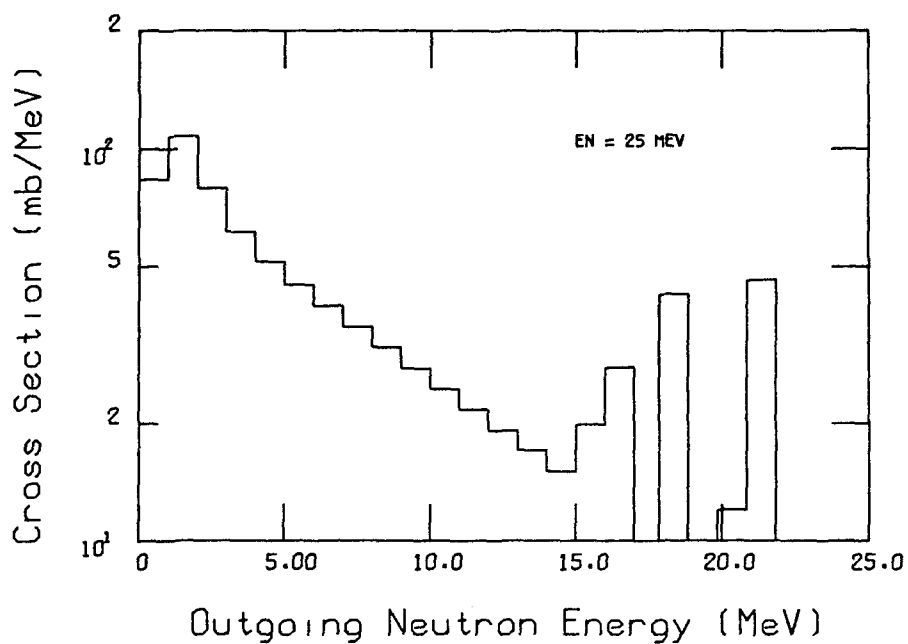


Figure 5. Calculated Neutron Emission Spectra for Incident Energies of 20 and 25 MeV

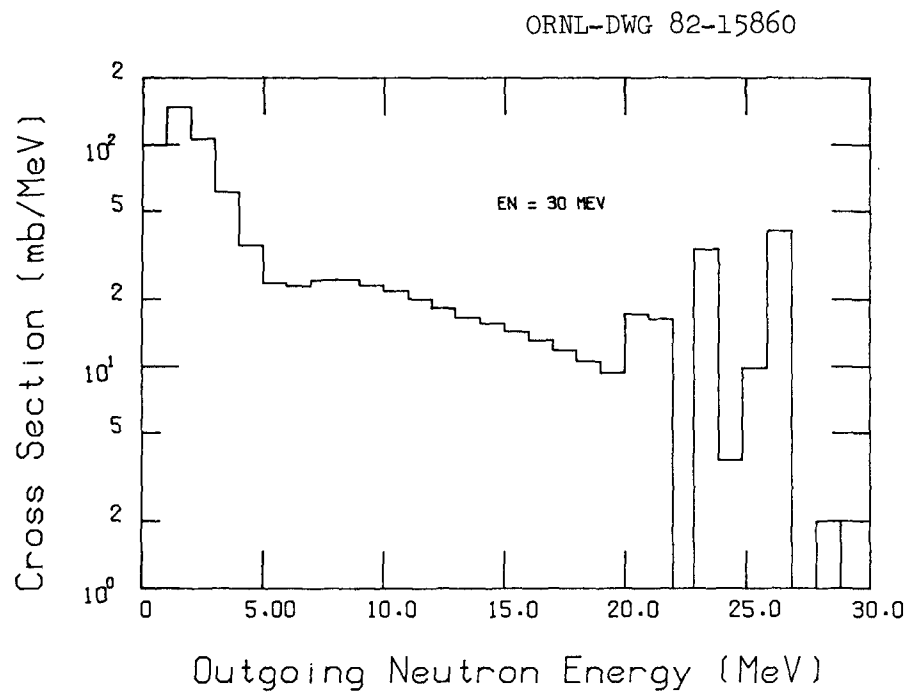
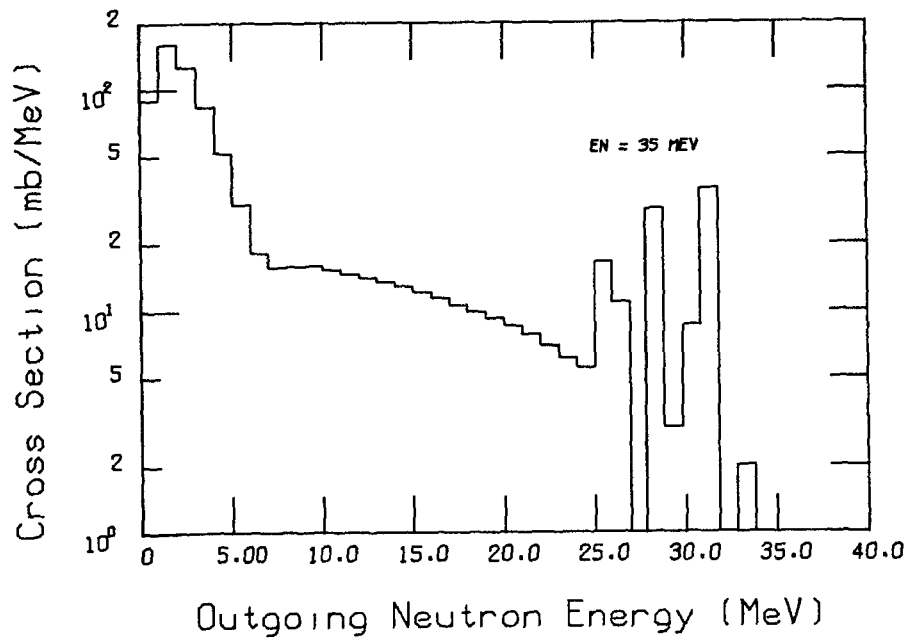


Figure 6. Calculated Neutron Emission Spectrum for Incident Energy of 30 MeV

ORNL-DWG 82-15861



ORNL-DWG 82-15862

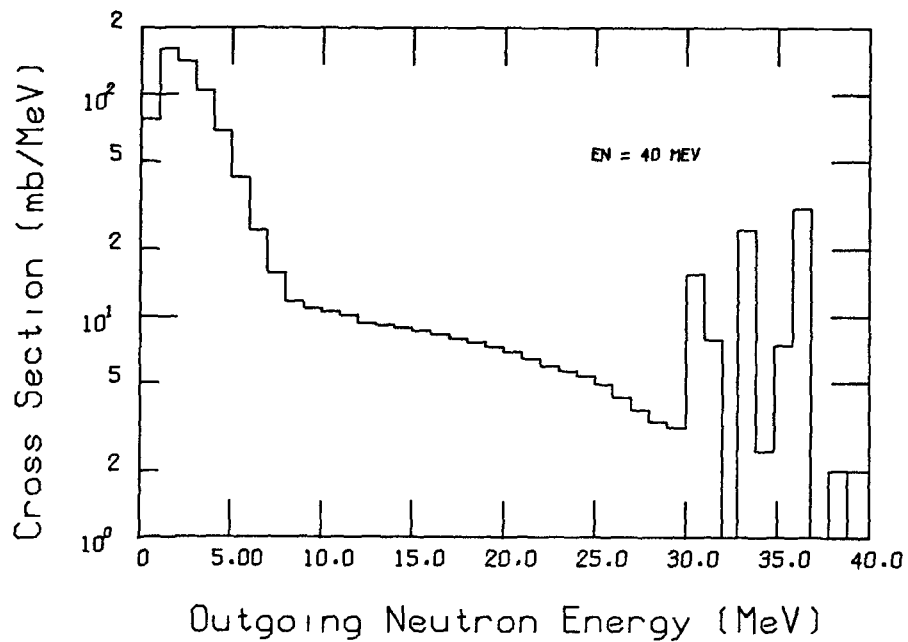
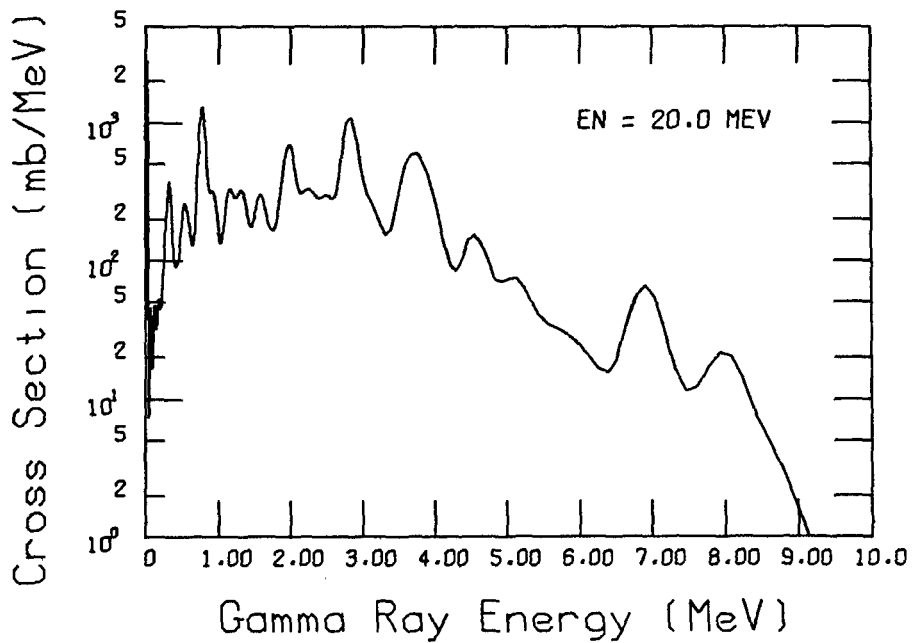


Figure 7. Calculated Neutron Emission Spectra for Incident Energies of 35 and 40 MeV

ORNL-DWG 82-15863



ORNL-DWG 82-15864

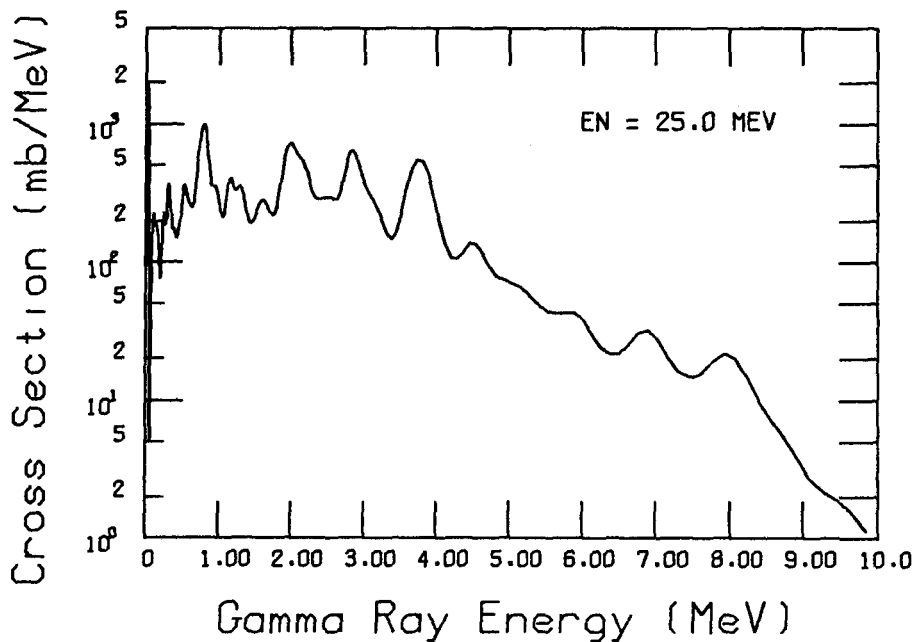
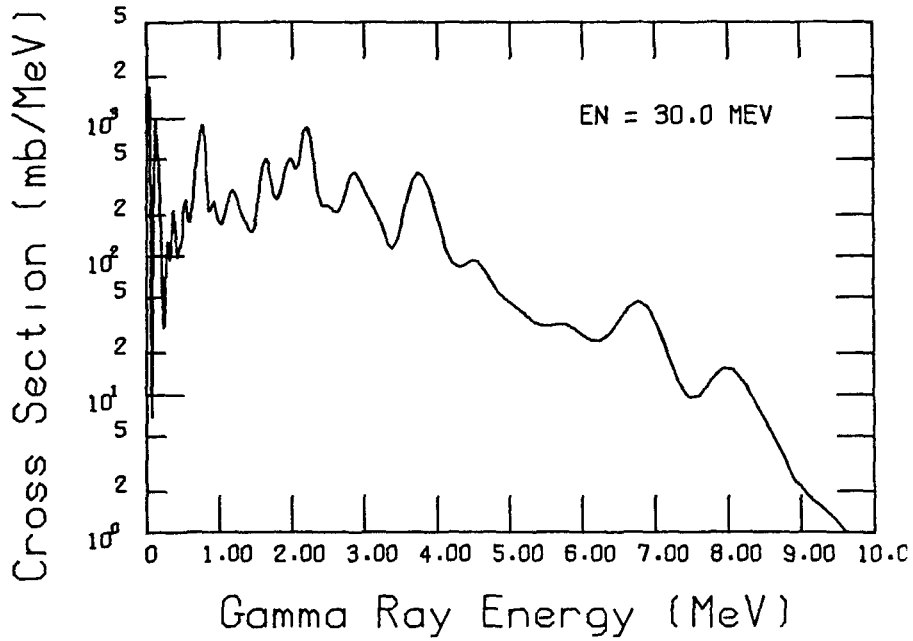


Figure 8. Calculated Gamma-Ray-Production Cross Sections for Incident Energies of 20 and 25 MeV

ORNL-DWG 82-15865



ORNL-DWG 82-15866

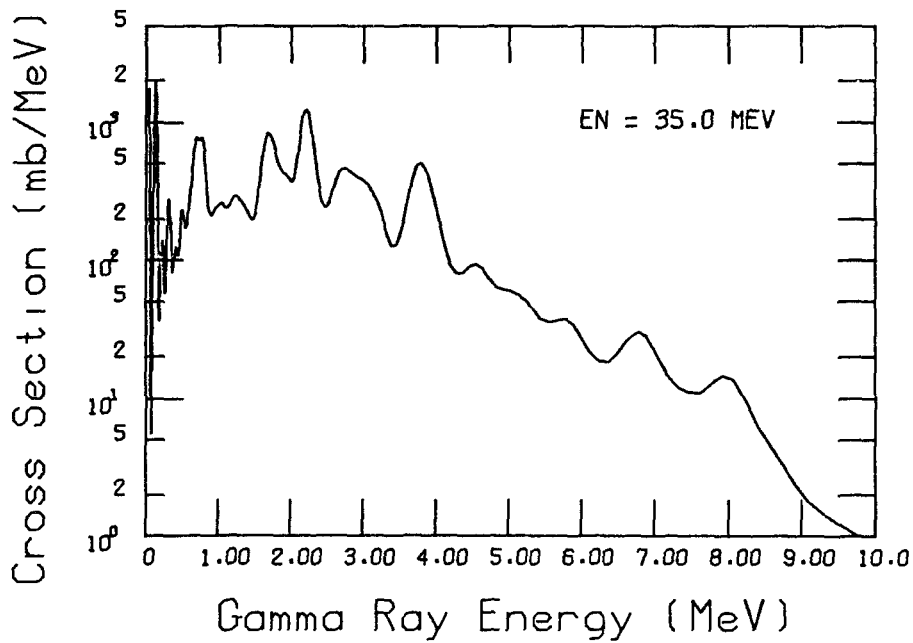


Figure 9. Calculated Gamma-Ray Production Cross Sections for Incident Energies of 30 and 35 MeV



ORNL-DWG 82-15867

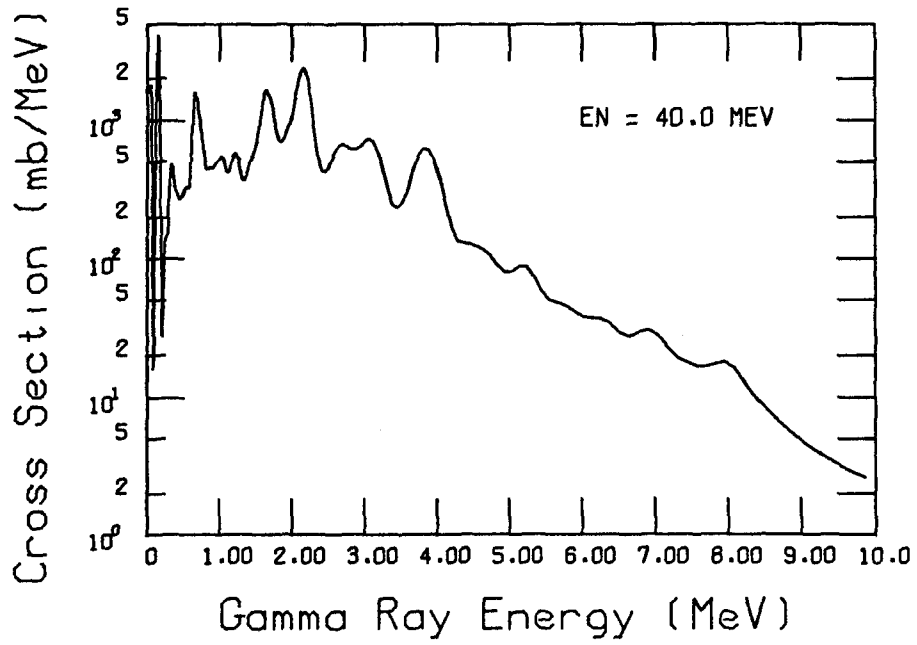
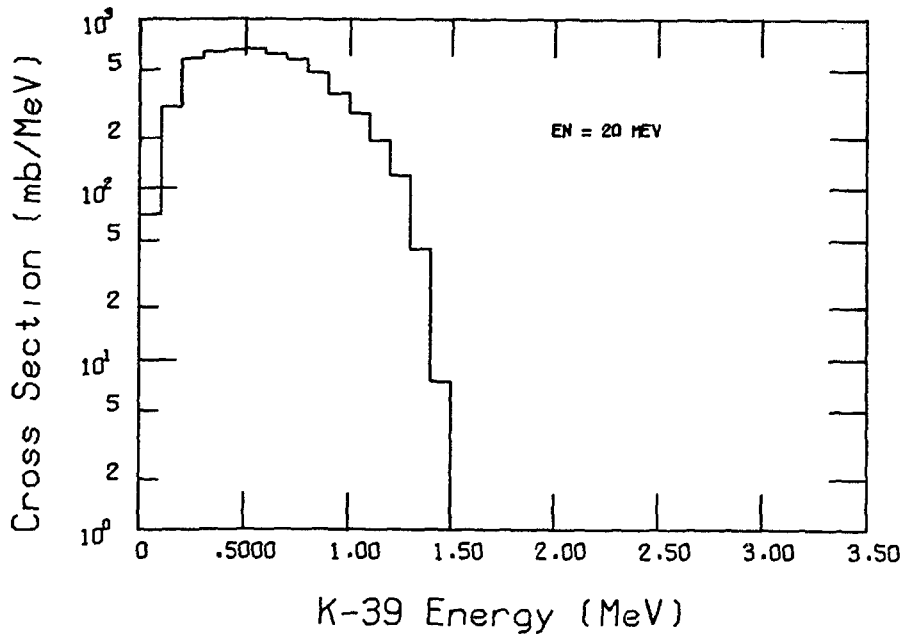


Figure 10. Calculated Gamma-Ray-Production Cross Sections for Incident Energy of 40 MeV

ORNL-DWG 82-15868



ORNL-DWG 82-15869

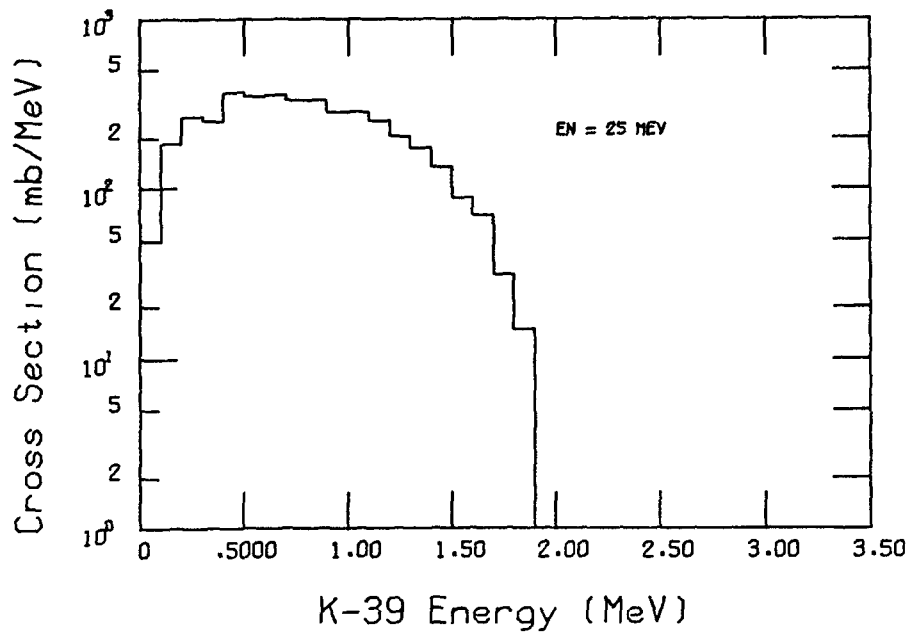
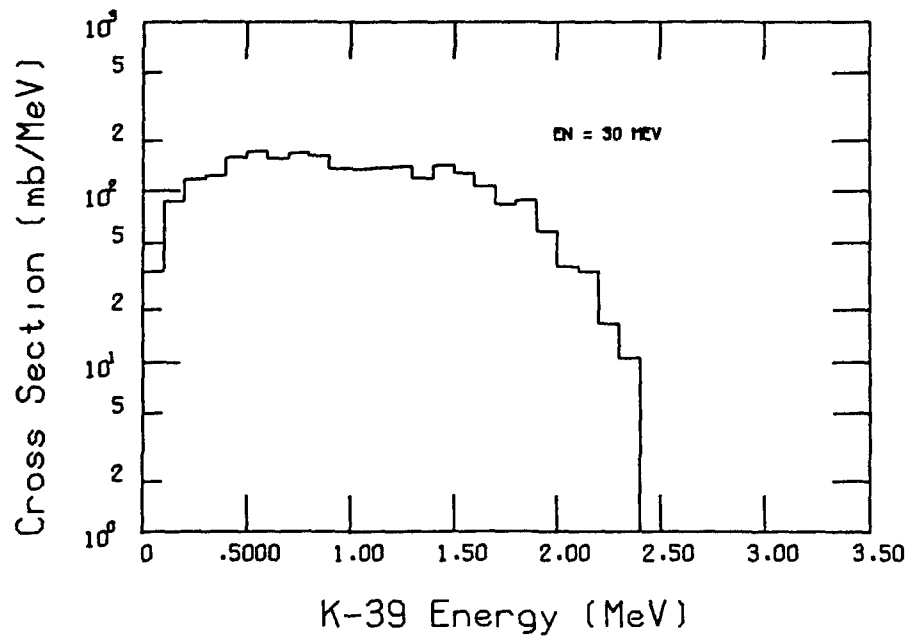


Figure 11. Calculated Recoil Spectra ( $^{39}\text{K}$  residual) for Incident Energies of 20 and 25 MeV

ORNL-DWG 82-15870



ORNL-DWG 82-15871

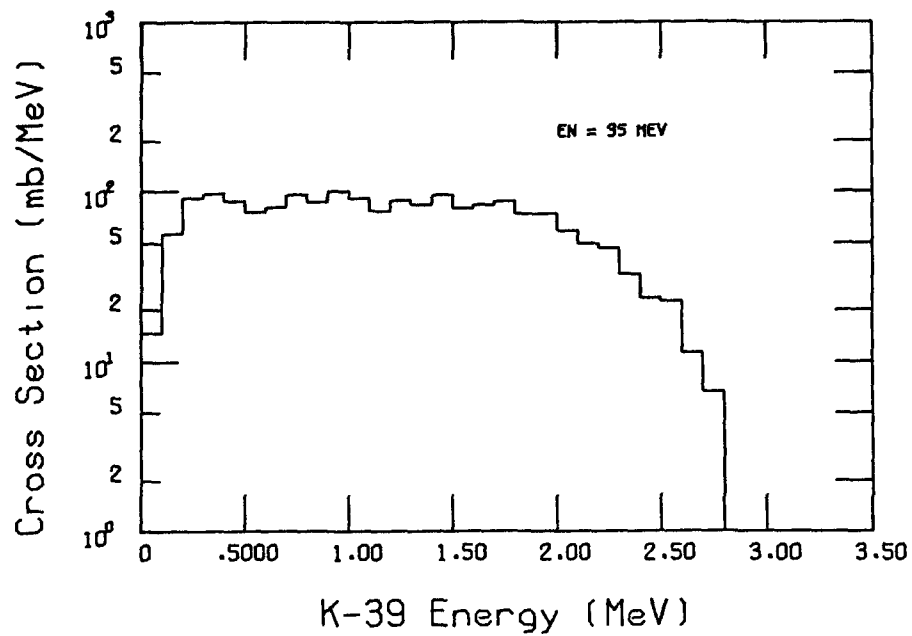


Figure 12. Calculated Recoil Spectra (<sup>39</sup>K residual) for Incident Energies of 30 and 35 MeV

ORNL-DWG 82-15872

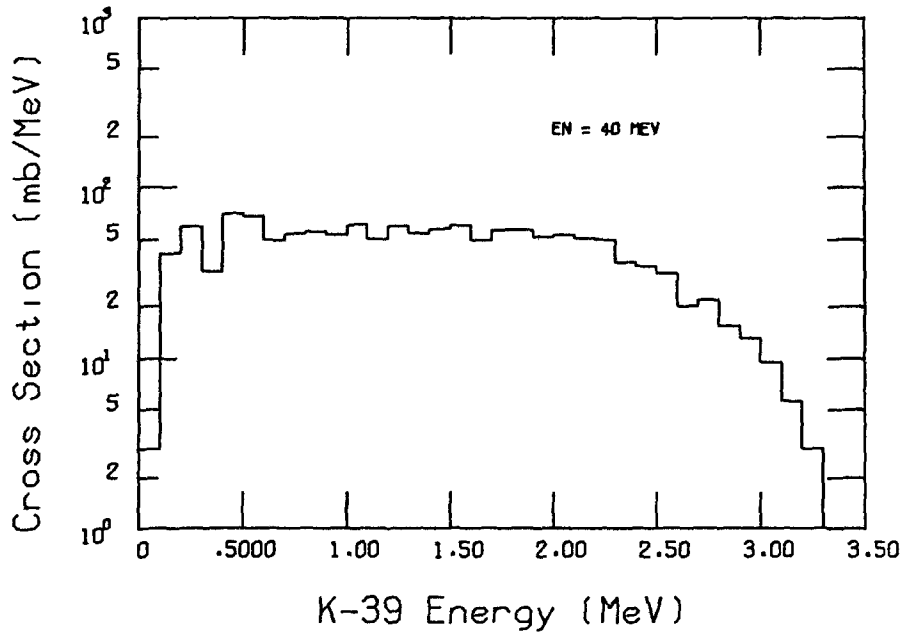


Figure 13. Calculated Recoil Spectra ( $^{39}\text{K}$  residual) for Incident Energy of 40 MeV

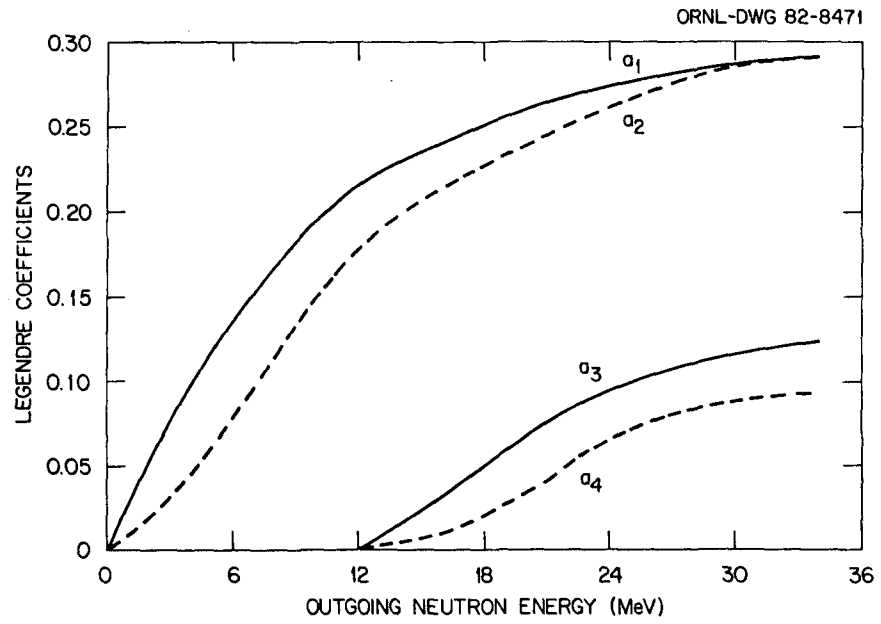


Figure 14. Legendre Coefficients of the Calculated Angular Distributions for the First Outgoing Neutron in (n,nx) Reaction for Incident Energies Between 20 and 40 MeV



## V. THE EVALUATED FILE

The calculated cross sections described here were compiled into a data file using the new proposed ENDF format<sup>3</sup>. The file includes data for the range of incident energies from 20 to 40 MeV only. Care was taken to ensure continuity with the previous evaluation<sup>2</sup> at 20 MeV for the reaction cross sections. This new evaluation depends completely on calculated results except for the total cross section.<sup>9</sup> The new format does not have any provisions for including the total cross section. However, the file does include the integrated elastic cross section which was derived by subtracting the calculated nonelastic cross section from the total cross section. Thus, the total cross section could be recomputed.

### Reaction Type Labels

As usual, the evaluation starts with a specification of the target and incident particle and with descriptive comments on the evaluation in a file with MF number 1 and MT number 451. Under the new format, individual reaction cross sections were filed with the MF number 53, total product yields or multiplicities with MF number 54, and normalized distributions in angle and energy for each product with MF number 55<sup>3</sup>. With the exception of elastic scattering and discrete inelastic scattering (see below), the continuum energy-angle distribution format (LAW=1)<sup>3</sup> was used for file 55. The new ENDF reaction labels (MT numbers) used in the file are shown in Table 15 along with the Q-values. Comments are now given for each reaction.

Table 15. Reactions With Their Q-Values and New Descriptors

Reaction Description	Q (MeV)	MT
(n,2n)	-10.028	651
(n,np)	-8.330	652
(n,n $\alpha$ )	-7.040	656
Sum of Reactions <sup>a</sup>	77.777 <sup>b</sup>	678
Elastic	0.000	680
(n,n') discrete	-1.158 to -7.114	681-697
(n,n') continuum	-7.63	698
Sum of (n,n') discrete and continuum <sup>c</sup>	77.777 <sup>b</sup>	699
(n,p)	-0.525	718
(n,d)	-6.019	738
(n,t)	-12.933	758
(n, <sup>3</sup> He)	-6.991	778
(n, $\alpha$ )	1.749	798

<sup>a</sup>Sum of (n,2 $\alpha$ ), (n, $\alpha$ p), (n,3n), (n,2np), (n,2n $\alpha$ ), (n,n2 $\alpha$ ), (n,n2p), (n,np $\alpha$ ), (n, $\alpha$ 2p), (n,p2 $\alpha$ ), (n,3 $\alpha$ ), and (n,2p).

<sup>b</sup>The Q value is not well defined.

<sup>c</sup>The sum of (n,n') discrete and (n,n') continuum was needed since the gamma-ray production for the levels and continuum was added together for file 55.



(n,2n) Reaction

The calculated (n,2n) cross sections are included in file 53 under the MT number 651. File 54 contains simple constant yields for the neutron and  $^{39}\text{Ca}$  residual, and energy-dependent yields based on the calculated gamma-ray spectra for the gamma rays. Calculated normalized distributions for each product are given in file 55, with angular distributions given for the outgoing neutrons. The Legendre coefficients from Fig. 14, used for the calculations in file 55, were weighted by the ratio  $\sigma(n,2n)/[2\sigma(n,2n)]$ . Recall that the angular distribution of the second outgoing neutron was assumed to be isotropic.

(n,np) Reaction

The calculated (n,np) + (n,pn) cross sections are included in file 53 under the MT number 652. Simple constant yields for the neutron, proton, and  $^{39}\text{K}$  residual, and energy-dependent yields based on the calculated gamma-ray spectra for the gamma rays, are all given in file 54. File 55 contains calculated normalized distributions for each product, with angular distributions given only for the outgoing neutrons. The Legendre coefficients from Fig. 14 were weighted by the ratio  $\sigma(n,np)/[\sigma(n,np) + \sigma(n,pn)]$ .

(n,n $\alpha$ ) Reaction

File 53 contains the computed (n,n $\alpha$ ) + (n, $\alpha$ n) cross sections under MT number 656. Simple constant yields for the neutron, alpha, and  $^{36}\text{Ar}$  residual, and energy-dependent yields based on the calculated gamma-ray spectra for the gamma rays are included in file 54. Computed normalized distributions for each product are given in file 55. The angular distributions are given only for the outgoing neutrons with the Legendre coefficients from Fig. 14 being weighted with the ratio  $\sigma(n,n\alpha)/[\sigma(n,n\alpha) + (n,\alpha n)]$ .

Sum of Reactions

The product form identifier MT 678 was used to lump together calculations of the complex reactions (n,2 $\alpha$ ), (n, $\alpha$ p), (n,3n), (n,2np), (n,2n $\alpha$ ), (n,n2 $\alpha$ ), (n,n2p), (n,np $\alpha$ ), (n, $\alpha$ 2p), (n,p2 $\alpha$ ), (n,3 $\alpha$ ), and (n,2p) (see Section IV). Calculated energy-dependent yields for the neutron, proton, alpha, and gamma were included under file 54. Also, for the recoil, a simple constant yield for the  $^{38}\text{Ar}$  residual was used in this section. That is,  $^{40}\text{Ca}$  (n,n2p) $^{38}\text{Ar}$  was used as the representative reaction for the computed recoil distribution given in file 55. All products were assumed to be isotropic in the center-of-mass system.

Elastic

The integrated elastic scattering cross section was derived by subtracting the sum of the nonelastic cross section from the measured<sup>9</sup> total cross section. These cross sections were entered into file 53 with MT number 680. File 54 contains simple constant yields for the neutron and  $^{40}\text{Ca}$  residual. The two-body format (LAW=2)<sup>3</sup> was used to enter the Legendre coefficients into file 55. The coefficients were obtained by fitting the angular distributions obtained with the optical potential given in Table 1.

(n,n') Discrete

Calculated cross sections from discrete inelastic scattering are included in file 53 under the MT numbers 681 to 697. Because the new format restricted the number of levels to 17, a number of levels had to be grouped together to be included in the file (see Table 3 of Ref. 2). Simple constant yields for the neutron and  $^{40}\text{Ca}$  residual were included in file 54 for each level. The two-body format (LAW=2)<sup>3</sup> was used to enter the Legendre coefficients, computed by the DWUCK<sup>15</sup> program (see Section II) for each level, into file 55.

(n,n') Continuum

Cross sections from inelastic scattering exciting the continuum are found in file 53 under MT number 698. Simple constant yields are given for the neutron and  $^{40}\text{Ca}$  residual in file 54. Angular distributions are given for the outgoing neutron in file 55. The Legendre coefficients entered in file 55 are as shown in Fig. 14. The  $^{40}\text{Ca}$  residual is assumed to be isotropic in the center-of-mass system.

Sum of (n,n') Discrete and Continuum

The sum of (n,n') discrete and continuum cross sections are included in file 53 under MT number 699. They must not be added in when computing the total cross section (by summing the partial cross sections), unless the files with MT numbers 681 to 698 are ignored. This file was needed since the gamma-ray production for the discrete levels and the continuum are calculated together by the TNG1 code.<sup>4</sup> Thus, normalized distributions for the gamma rays from inelastic scattering will be found in file 55 under MT number 699. The energy-dependent yield based on the calculated gamma-ray spectra is found in file 54.

(n,p) Reaction

File 53 contains computed (n,p) cross sections under MT number 718. Simple constant yields for the proton and  $^{39}\text{K}$  residual and energy-dependent yields based on the computed gamma-ray spectra for the gamma rays are given in file 54. Calculated normalized distributions for each product, all assumed isotropic in the center-of-mass system, are contained in file 55.

(n, $\alpha$ ) Reaction

The computed (n, $\alpha$ ) cross sections are given in file 53 using the MT number 798. File 54 contains constant yields for the alpha and  $^{37}\text{Ar}$  residual and energy-dependent yields for the gamma rays. File 55 contains the normalized distributions for each product which are assumed isotropic in the center-of-mass system.

(n,d), (n,t), and (n, $^3\text{He}$ ) Reactions

The cross sections for the (n,d), (n,t), and (n, $^3\text{He}$ ) reactions were found simply by extending the curve in the previous evaluation for incident energies to 20 MeV.<sup>2</sup> For the (n,d) and (n,t) reactions, the energy-dependent yields used for the gamma rays in file 54 (sections 738 and 758, respectively) were the same as calculated for the (n,p) reaction (section 718). The energy-dependent yields for the gamma rays used for the (n, $^3\text{He}$ ) reaction (section 778) were the same as computed for the (n, $\alpha$ ) reaction (section 798). The other products for these reactions used simple constant yields in file 54. Likewise, the normalized distributions given in file 55 for the (n,d) and (n,t) reactions are the same as calculated for the (n,p) reaction; the (n, $^3\text{He}$ ) reaction has the same distributions as the (n, $\alpha$ ) reaction. All products are assumed isotropic in the center-of-mass system.

Example of Format

To describe the new file format further, we have included in the Appendix parts of the evaluated file for the (n,np) reaction (MT=652). It will be helpful to review the new format rules<sup>3</sup> while looking at this Appendix. The entire sections for files 53 and 54 for this reaction are shown. However, only parts of file 55 are given to conserve space, but enough is included to show what the new format is like. The entire file is at the National Nuclear Data Center at Brookhaven National Laboratory.



## VI. SUMMARY

This report has presented the nuclear models and parameters used in computing neutron-induced reactions on  $^{40}\text{Ca}$  between 20 and 40 MeV. The calculations were made using the multistep Hauser-Feshbach model code TNG1<sup>4</sup>. Care was taken to ensure continuity with the previous evaluation for  $^{40}\text{Ca}$  to 20 MeV<sup>2</sup>. Input parameters for TNG1, including optical model sets, discrete level information, level-density parameters, and direct reaction model parameters, were discussed. The resulting cross section sets are consistent and energy balance is ensured. Calculated results were judged reasonable and are shown in the report.

The computed data were combined into an ENDF evaluation file using the new charged-particle format<sup>3</sup>. The new reaction type labels were given along with discussions for each reaction. This evaluated file has been transmitted to the National Nuclear Data Center at Brookhaven National Laboratory.





## REFERENCES

1. C. R. Head, "Nuclear Data Requirements of the Magnetic Fusion Power Program of the United States of America," presented at the IAEA Advisory Group Meeting on Nuclear Data for Fusion Reactor Technology, Vienna, Austria (December 11-15, 1978).
2. D. M. Hetrick and C. Y. Fu, "A Calculation of Neutron and Gamma-Ray Production Cross Sections for Calcium from 8 to 20 MeV," ORNL/TM-7752, ENDF-308 (1981).
3. R. E. MacFarlane, "ENDF/B Format for Charged Particle Reactions," adopted for use by the Cross Section Evaluation Working Group, to be published.
4. C. Y. Fu, "A Consistent Nuclear Model for Compound and Precompound Reactions with Conservation of Angular Momentum," ORNL/TM-7042 (1980).
5. C. Y. Fu, "Consistent Calculations of (n,x) and (n,x $\gamma$ ) Cross Sections for  $^{40}\text{Ca}$ ,  $E_n = 1-20$  MeV," Atomic Data and Nuclear Data Tables 17, 127 (1976).
6. J. Rapaport, V. Kulkarni, and R. W. Finlay, Nuclear Physics A330, 15 (1979).
7. R. P. DeVito, Ph.D. Thesis, Michigan State University, 1979 (unpublished).
8. G. C. Wick, Phys. Rev., 75, 1459 (1949).
9. D. C. Larson, J. A. Harvey, and N. W. Hill, Oak Ridge National Laboratory, 1980 (to be published).

10. F. G. Perey, Oak Ridge National Laboratory, unpublished.
11. C. R. Gruhn, T. Y. T. Kuo, C. J. Maggiore, H. McManus, F. Petrovich, and B. M. Freedom, Phys. Rev., C6, 915 (1972).
12. M. P. Fricke, E. E. Gross, B. J. Morton, and A. Zucker, Phys. Rev., 156, 1207 (1967).
13. L. McFadden and G. R. Satchler, Nuclear Physics, 84, 177 (1966).
14. P. M. Endt and C. Van der Leun, Nuclear Physics, A310, 1 (1978).
15. P. D. Kunz, University of Colorado, unpublished.
16. A. Gilbert and A. G. W. Cameron, Can. J. Physics, 43, 1446 (1965).
17. C. Y. Fu, "Development and Applications of Multistep Hauser-Feshbach/Pre-equilibrium Model Theory," Proc. Symp. on Neutron Cross Sections from 10 to 50 MeV, eds. M. R. Bhat and S. Pearlstein, BNL-NCS-51245 (1980).

APPENDIX

Example Listing of (n,np) Reaction in ENDF Format



2.0040E+04-3.7409E-02		0	0	0		0132053652	207
0.0000E-01-8.3300E+06		0	0	2		7132053652	208
3	2	7	4	0		0132053652	209
1.00000E-05	0.0000E-012.00000E+07	0.0000E-012.00000E+07	5.6000E-01	132053652		210	210
2.50000E+07	4.0033E-013.00000E+07	2.5395E-013.50000E+07	1.8661E-01	132053652		211	211
4.00000E+07	1.3805E-010.00000E-01	0.0000E-010.00000E-01	0.0000E-01	132053652		212	212
				132053	0	213	213
2.0040E+04-3.7409E-02		0	0	4		3132054652	423
1.0000E+00	1.0000E+00	0	10	0		0132054652	424
1.0010E+03	1.0000E+00	0	10	0		0132054652	425
1.9039E+04	1.0000E+00	0	10	0		0132054652	426
0.0000E-01	0.0000E-01	0	10	1		7132054652	427
7	2	0	0	0		0132054652	428
1.0000E-05	0.0000E-01	2.0000E+07	0.0000E-01	2.0000E+07	1.0023E+00	132054652	429
2.5000E+07	1.4366E+00	3.0000E+07	1.2584E+00	3.5000E+07	1.2832E+00	132054652	430
4.0000E+07	1.1592E+00	0.0000E-01	0.0000E-01	0.0000E-01	0.0000E-01	132054652	431
						132054	0
							432
2.0040E+04-3.7409E-02		0	2	4		0132055652	863
1.0000E+00	0.0000E-01	0	1	0		0132055652	864
0.0000E-01	0.0000E-01	2	1	1		7132055652	865
7	12	0	0	0		0132055652	866
0.0000E-01	1.0000E-05	0	0	4		2132055652	867
0.0000E-01	1.0000E+00	1.0000E+00	0.0000E-01	0.0000E-01	0.0000E-01	132055652	868
0.0000E-01	2.0000E+07	0	0	4		2132055652	869
0.0000E-01	1.0000E+00	1.0000E+00	0.0000E-01	0.0000E-01	0.0000E-01	132055652	870
	2.0000E+07			138		23132055652	871
0.0000E-01	7.8030E-08	0.0000E-01	0.0000E-01	0.0000E-01	0.0000E-01	132055652	872
5.0000E+05	1.6043E-07	1.3755E-09	4.6766E-10	0.0000E-01	0.0000E-01	132055652	873
1.0000E+06	1.7392E-07	2.9822E-09	1.0140E-09	0.0000E-01	0.0000E-01	132055652	874
1.5000E+06	1.8005E-07	4.6310E-09	1.5746E-09	0.0000E-01	0.0000E-01	132055652	875
2.0000E+06	1.7629E-07	6.0458E-09	2.0556E-09	0.0000E-01	0.0000E-01	132055652	876
1.0500E+07	9.1134E-09	1.2486E-09	9.7981E-10	0.0000E-01	0.0000E-01	132055652	893
1.1000E+07	0.0000E-01	0.0000E-01	0.0000E-01	0.0000E-01	0.0000E-01	132055652	894
	2.5000E+07			138		23132055652	895
0.0000E-01	7.9880E-08	0.0000E-01	0.0000E-01	0.0000E-01	0.0000E-01	132055652	896
7.0000E+05	1.2624E-07	1.7008E-09	5.7826E-10	0.0000E-01	0.0000E-01	132055652	897
1.4000E+06	9.3726E-08	2.5255E-09	8.5866E-10	0.0000E-01	0.0000E-01	132055652	898
2.1000E+06	7.6440E-08	3.0895E-09	1.0828E-09	0.0000E-01	0.0000E-01	132055652	899
1.4700E+07	2.4418E-08	4.3521E-09	3.8278E-09	3.6610E-10	1.2689E-10	132055652	917
1.5400E+07	0.0000E-01	0.0000E-01	0.0000E-01	0.0000E-01	0.0000E-01	132055652	918
	3.0000E+07			162		27132055652	919
0.0000E-01	7.2104E-08	0.0000E-01	0.0000E-01	0.0000E-01	0.0000E-01	132055652	920

8.0000E+05	1.0919E-07	1.7371E-09	5.9060E-10	0.0000E-01	0.0000E-01	1132055652	921
1.6000E+06	6.1638E-08	1.9611E-09	6.6679E-10	0.0000E-01	0.0000E-01	1132055652	922
2.4000E+06	3.9425E-08	1.8816E-09	7.0873E-10	0.0000E-01	0.0000E-01	1132055652	923
⋮							
2.0000E+07	2.8172E-08	5.8263E-09	5.3408E-09	1.4902E-09	7.3949E-10	132055652	945
2.0800E+07	0.0000E-01	0.0000E-01	0.0000E-01	0.0000E-01	0.0000E-01	01132055652	946
	3.5000E+07			174	29132055652		947
0.0000E-01	6.0760E-08	0.0000E-01	0.0000E-01	0.0000E-01	0.0000E-01	01132055652	948
9.0000E+05	7.3269E-08	1.3463E-09	4.5776E-10	0.0000E-01	0.0000E-01	01132055652	949
1.8000E+06	4.9845E-08	1.8318E-09	6.2282E-10	0.0000E-01	0.0000E-01	01132055652	950
2.7000E+06	2.4962E-08	1.3761E-09	5.4634E-10	0.0000E-01	0.0000E-01	01132055652	951
⋮							
2.4300E+07	2.3952E-08	5.2226E-09	5.0327E-09	1.8710E-09	1.3174E-09	132055652	975
2.5200E+07	0.0000E-01	0.0000E-01	0.0000E-01	0.0000E-01	0.0000E-01	01132055652	976
	4.0000E+07			174	29132055652		977
0.0000E-01	4.7376E-08	0.0000E-01	0.0000E-01	0.0000E-01	0.0000E-01	01132055652	978
1.0000E+06	7.1288E-08	1.4640E-09	4.9775E-10	0.0000E-01	0.0000E-01	01132055652	979
2.0000E+06	4.3882E-08	1.8023E-09	6.1279E-10	0.0000E-01	0.0000E-01	01132055652	980
3.0000E+06	1.7163E-08	1.0574E-09	4.3705E-10	0.0000E-01	0.0000E-01	01132055652	981
⋮							
2.9000E+07	1.9805E-08	4.4861E-09	4.4495E-09	1.8424E-09	1.3910E-09	132055652	1005
3.0000E+07	0.0000E-01	0.0000E-01	0.0000E-01	0.0000E-01	0.0000E-01	01132055652	1006
1.0010E+03	0.0000E-01	0	1	0	0	0132055652	1007
0.0000E-01	0.0000E-01	2	1	1	1	7132055652	1008
	7	12	0	0	0	0132055652	1009
0.0000E-01	1.0000E-05	0	0	4	4	2132055652	1010
0.0000E-01	1.0000E+00	1.0000E+00	0.0000E-01	0.0000E-01	0.0000E-01	01132055652	1011
0.0000E-01	2.0000E+07	0	0	4	4	2132055652	1012
0.0000E-01	1.0000E+00	1.0000E+00	0.0000E-01	0.0000E-01	0.0000E-01	01132055652	1013
	2.0000E+07			48	24132055652		1014
0.0000E-01	0.0000E-01	5.0000E+05	7.5379E-09	1.0000E+06	2.8862E-08	132055652	1015
1.5000E+06	5.5969E-08	2.0000E+06	1.0630E-07	2.5000E+06	1.6203E-07	132055652	1016
⋮							
1.0500E+07	2.6213E-08	1.1000E+07	2.0183E-08	1.1500E+07	0.0000E-01	1132055652	1022
	2.5000E+07			48	24132055652		1023
0.0000E-01	0.0000E-01	7.0000E+05	9.9654E-10	1.4000E+06	0.0000E-01	1132055652	1024
2.1000E+06	6.5353E-08	2.8000E+06	1.4928E-07	3.5000E+06	1.9798E-07	132055652	1025
⋮							
1.4700E+07	1.5353E-08	1.5400E+07	1.4294E-08	1.6100E+07	0.0000E-01	1132055652	1031
	3.0000E+07			52	26132055652		1032
0.0000E-01	0.0000E-01	2.4000E+06	6.0994E-08	3.2000E+06	1.4510E-07	132055652	1033
4.0000E+06	1.7604E-07	4.8000E+06	1.5696E-07	5.6000E+06	1.3255E-07	132055652	1034
⋮							

2.0800E+07	1.1950E-08	2.1600E+07	0.0000E-01	2.2400E+07	0.0000E-01	1132055652	1041
	3.5000E+07				56	28132055652	1042
0.0000E-01	0.0000E-01	2.7000E+06	7.9543E-08	3.6000E+06	1.7186E-07	132055652	1043
4.5000E+06	1.6717E-07	5.4000E+06	1.3188E-07	6.3000E+06	1.0259E-07	132055652	1044
⋮							
2.6100E+07	0.0000E-01	2.7000E+07	0.0000E-01	2.7900E+07	0.0000E-01	1132055652	1052
	4.0000E+07				60	30132055652	1053
0.0000E-01	0.0000E-01	3.0000E+06	1.0820E-07	4.0000E+06	1.6954E-07	132055652	1054
5.0000E+06	1.3535E-07	6.0000E+06	1.0281E-07	7.0000E+06	8.2526E-08	132055652	1055
⋮							
2.9000E+07	1.1782E-08	3.0000E+07	1.0769E-08	3.1000E+07	0.0000E-01	1132055652	1063
1.9039E+04	0.0000E-01	0	1	0		0132055652	1064
0.0000E-01	0.0000E-01	2	1	1		7132055652	1065
	7	12	0	0	0	0132055652	1066
0.0000E-01	1.0000E-05	0	0	4		2132055652	1067
0.0000E-01	1.0000E+00	1.0000E+00	0.0000E-01	0.0000E-01	0.0000E-01	1132055652	1068
0.0000E-01	2.0000E+07	0	0	4		2132055652	1069
0.0000E-01	1.0000E+00	1.0000E+00	0.0000E-01	0.0000E-01	0.0000E-01	1132055652	1070
	2.0000E+07			32		16132055652	1071
0.0000E-01	1.2590E-07	1.0000E+05	5.4451E-07	2.0000E+05	1.0496E-06	132055652	1072
3.0000E+05	1.1479E-06	4.0000E+05	1.1646E-06	5.0000E+05	1.1883E-06	132055652	1073
⋮							
1.5000E+06	0.0000E-01	1.6000E+06	0.0000E-01	1.7000E+06	0.0000E-01	1132055652	1077
	2.5000E+07			40		20132055652	1078
0.0000E-01	1.2144E-07	1.0000E+05	4.6402E-07	2.0000E+05	6.6536E-07	132055652	1079
3.0000E+05	6.2167E-07	4.0000E+05	9.2340E-07	5.0000E+05	8.6963E-07	132055652	1080
⋮							
1.8000E+06	3.7111E-08	1.9000E+06	0.0000E-01	2.0000E+06	0.0000E-01	1132055652	1085
	3.0000E+07			50		25132055652	1086
0.0000E-01	1.3225E-07	1.0000E+05	3.4294E-07	2.0000E+05	4.6309E-07	132055652	1087
3.0000E+05	4.8837E-07	4.0000E+05	6.2045E-07	5.0000E+05	6.6996E-07	132055652	1088
⋮							
2.4000E+06	0.0000E-01	2.5000E+06	0.0000E-01	2.6000E+06	0.0000E-01	1132055652	1095
	3.5000E+07			60		30132055652	1096
0.0000E-01	7.8586E-08	1.0000E+05	3.0465E-07	2.0000E+05	4.9159E-07	132055652	1097
3.0000E+05	5.2267E-07	4.0000E+05	4.6796E-07	5.0000E+05	4.0311E-07	132055652	1098
⋮							
2.7000E+06	3.5343E-08	2.8000E+06	5.2346E-09	2.9000E+06	0.0000E-01	1132055652	1106
	4.0000E+07			68		34132055652	1107
0.0000E-01	2.1178E-08	1.0000E+05	2.9852E-07	2.0000E+05	4.2947E-07	132055652	1108
3.0000E+05	2.3185E-07	4.0000E+05	5.1118E-07	5.0000E+05	4.9201E-07	132055652	1109

```

      .
      .
3.3000E+06 0.0000E-01 3.4000E+06 0.0000E-01 3.5000E+06 0.0000E-01 132055652 1119
0.0000E-01 0.0000E-01          0          1          0          0132055652 1120
0.0000E-01 0.0000E-01          2          1          1          7132055652 1121
      7      12          0          0          0          0132055652 1122
0.0000E-01 1.0000E-05          0          0          4          2132055652 1123
0.0000E-01 1.0000E+00 1.0000E+00 0.0000E-01 0.0000E-01 0.0000E-01 132055652 1124
0.0000E-01 2.0000E+07          0          0          4          2132055652 1125
0.0000E-01 1.0000E+00 1.0000E+00 0.0000E-01 0.0000E-01 0.0000E-01 132055652 1126
      2.0000E+07          344          172132055652 1127
0.0000E-01 0.0000E-01 1.5000E+05 3.2042E-08 2.0000E+05 3.2043E-08 132055652 1128
2.5000E+05 6.0044E-08 3.0000E+05 6.7638E-07 3.5000E+05 6.0044E-08 132055652 1129
      .
      .
8.6500E+06 0.0000E-01 8.7000E+06 0.0000E-01 8.7500E+06 0.0000E-01 132055652 1185
      2.5000E+07          320          160132055652 1186
0.0000E-01 1.5189E-08 7.0000E+04 1.5189E-08 1.4000E+05 5.5064E-08 132055652 1187
2.1000E+05 4.7494E-08 2.8000E+05 3.9973E-07 3.5000E+05 1.0367E-07 132055652 1188
      .
      .
1.1130E+07 0.0000E-01 1.1200E+07 0.0000E-01 1.1270E+07 0.0000E-01 132055652 1240
      3.0000E+07          284          142132055652 1241
0.0000E-01 1.9620E-08 8.0000E+04 1.9620E-08 1.6000E+05 5.8867E-08 132055652 1242
2.4000E+05 4.9056E-08 3.2000E+05 2.8749E-07 4.0000E+05 9.6278E-08 132055652 1243
      .
      .
1.1280E+07 0.0000E-01 1.1360E+07 0.0000E-01 1.1440E+07 0.0000E-01 132055652 1289
      3.5000E+07          254          127132055652 1290
0.0000E-01 2.6563E-08 9.0000E+04 2.6563E-08 1.8000E+05 1.3489E-08 132055652 1291
2.7000E+05 2.4147E-07 3.6000E+05 5.0214E-08 4.5000E+05 7.2722E-08 132055652 1292
      .
      .
1.1340E+07 0.0000E-01 1.1430E+07 0.0000E-01 1.1520E+07 0.0000E-01 132055652 1333
      4.0000E+07          234          117132055652 1334
0.0000E-01 0.0000E-01 1.0000E+05 2.5102E-08 2.0000E+05 2.5107E-08 132055652 1335
3.0000E+05 2.2451E-07 4.0000E+05 2.5107E-08 5.0000E+05 1.7501E-07 132055652 1336
      .
      .
1.1400E+07 2.8361E-10 1.1500E+07 2.8361E-10 1.1600E+07 0.0000E-01 132055652 1373
      132055 0 1374

```



INTERNAL DISTRIBUTION

- |        |   |        |   |
|--------|---|--------|---|
| 1.     | R. G. Alsmiller, Jr.                              | 25.    | M. R. Patterson   |
| 2.     | H. P. Carter/G. E. Whitesides/<br>CS X-10 Library | 26.    | R. W. Peelle  |
| 3.     | J. K. Dickens                                     | 27.    | R. W. Roussin   |
| 4-8.   | C. Y. Fu  | 28.    | R. T. Santoro   |
| 9.     | T. A. Gabriel                                     | 29.    | Central Research Library                                  |
| 10-14. | D. M. Hetrick                                     | 30.    | ORNL Y-12 Technical Library<br>Document Reference Section |
| 15-19. | D. C. Larson                                      | 31.    | K-25 Plant Library  |
| 20.    | N. M. Larson                                      | 32-33. | Laboratory Records<br>Department                          |
| 21.    | F. C. Maienschein                                 | 34.    | ORNL Patent Office  |
| 22.    | B. F. Maskewitz                                   | 35.    | Laboratory Records (RC)                                   |
| 23.    | G. S. McNeilly                                    |        |   |
| 24.    | B. D. Murphy                                      |        |   |

EXTERNAL DISTRIBUTION

36. E. D. Arthur, T-2, MS243, Los Alamos National Laboratory, P.O. Box 1663, Los Alamos, NM 87545.
37. S. E. Berk, G234, Division of Development and Technology Office of Fusion Energy, USDOE, Washington, DC 20545.
38. Chief, Mathematics and Geoscience Branch, DOE, Washington, DC 20545.
39. Herbert Goldstein, 211 Mudd Columbia University, 520 West 120th St., New York, NY 10027.
40. Robert MacFarlane, T-2, MS243, Los Alamos National Laboratory, P.O. Box 1663, Los Alamos, NM 87545.
41. F. M. Mann, W/A-4, Westinghouse Hanford, P.O. Box 1970, Richland, WA 99352.
42. J. N. Rogers, Division 8324, Sandia Laboratories, Livermore, CA 94550.
43. Robert Schenter, Westinghouse Hanford, P.O. Box 1970, Richland, WA 99352.
44. Stanley Whetstone, Division Nuclear Sciences, Office of Basic Energy Sciences, U.S. DOE, Washington, DC 20545.
45. Phillip Young, T-2, MS-243, Los Alamos National Laboratory, P.O. Box 1663, Los Alamos, NM 87545.
46. Office of Assistance Manager for Energy Research and Development, Department of Energy, Oak Ridge Operations, Oak Ridge, TN 37830.
- 47-136. April Donegain, National Nuclear Data Center, ENDF, Brookhaven National Laboratory, Upton, NY 11973
- 137-163. Technical Information Center, Oak Ridge, TN 37830

